1

2

3 **Ruxolitinib and polycation combination treatment overcomes multiple mechanisms of**

4 **resistance of pancreatic cancer cells to oncolytic vesicular stomatitis virus**

5

6

7 Sébastien A. Felt[1], Gaith N. Droby[1] and Valery Z. Grdzelishvili[1,*]

8

9 [1] Department of Biological Sciences, University of North Carolina at Charlotte,

10 Charlotte, North Carolina, United States.

11

12

13

14

15 vesicular stomatitis virus; oncolytic virus; pancreatic cancer; virus attachment; polycation;

16 polybrene; DEAE-dextran; type I interferon; ruxolitinib; resistance; combination treatment

17

18

19 * Corresponding author.

20 Mailing address: University of North Carolina at Charlotte, Department of Biological

21 Sciences, 9201 University City Blvd., Charlotte NC 28223, USA.

22 Phone: 704-687-7778, Fax: 704-687-1488. E-mail: vzgrdzel@uncc.edu

23   **ABSTRACT**

24   Vesicular stomatitis virus (VSV) is a promising oncolytic virus (OV). Although VSV is

25   effective against a majority of pancreatic ductal adenocarcinoma (PDAC) cell lines, some

26   PDAC cell lines are highly resistant to VSV, and the mechanisms of the resistance are still

27   unclear. JAK 1/2 inhibitors (such as ruxolitinib and JAK Inhibitor 1) strongly stimulate VSV

28   replication and oncolysis in all resistant cell lines, but only partially improve susceptibility of

29   resistant PDACs to VSV. VSV tumor tropism is generally dependent on the permissiveness

30   of malignant cells to viral replication, rather than on receptor specificity, with several

31   ubiquitously expressed cell-surface molecules to play a role in VSV attachment to host cells.

32   However, as VSV attachment to PDAC cells has never been tested before, here we

33   examined if it was possibly inhibited in resistant PDACs. Our data show a dramatically

34   weaker attachment of VSV to HPAF-II, the most resistant human PDAC cell line. Although

35   sequence analysis of LDLR mRNA did not reveal any amino acid substitutions in this cell

36   line, HPAF-II cells displayed the lowest level of LDLR expression and dramatically lower

37   LDL uptake. Treatment of cells with various statins strongly increased LDLR expression

38   levels, but did not improve VSV attachment or LDL uptake in HPAF-II. However, LDLR-

39   independent attachment of VSV to HPAF-II cells was dramatically improved by treating cells

40   with polybrene or DEAE-dextran. Moreover, combining VSV with ruxolitinib and polybrene or

41   DEAE-dextran successfully broke the resistance of HPAF-II to VSV by simultaneously

42   improving VSV attachment and replication.

43

44

45

46

47

IMPORTANCE

49 Oncolytic virus (OV) therapy is an anticancer approach that uses viruses that selectively

50 infect and kill cancer cells. This study focuses on oncolytic vesicular stomatitis virus (VSV)

51 against pancreatic ductal adenocarcinoma (PDAC). Although VSV is effective against most

52 PDACs, some are highly resistant to VSV, and the mechanisms are still unclear. Here we

53 examined if VSV attachment to cells was inhibited in resistant PDACs. Our data show very

54 inefficient attachment of VSV to the most resistant human PDAC cell line HPAF-II. However,

55 VSV attachment to HPAF-II cells was dramatically improved by treating cells with

56 polycations. Moreover, combining VSV with polycations and ruxolitinib (inhibits antiviral

57 signaling) successfully broke the resistance of HPAF-II to VSV by simultaneously improving

58 VSV attachment and replication. We envision that this novel triple combination approach

59 could be used in the future to treat PDAC tumors highly resistant to OV therapy.

60

61

INTRODUCTION

63 Oncolytic virus (OV) therapy is an anticancer approach that uses replication-competent

64 viruses that can selectively infect, replicate in, and kill cancer cells. Currently, three OVs are

65 approved for clinical use: herpes simplex virus 1 based T-VEC for melanoma, approved in

66 the U.S. (1) and later in the European Union (2), enteric cytopathic human orphan virus 7

67 based RIGVIR for melanoma, in Latvia, Georgia and Armenia (3), and adenovirus type 5

68 based Gendicine and Oncorine for head and neck squamous cell carcinoma in China (4).

69   This study focuses on vesicular stomatitis virus (VSV, a rhabdovirus), which has been used

70   successfully against many cancers in preclinical studies (5, 6), and is currently in a phase I

71   clinical trial against refractory solid tumors (ClinicalTrials.gov Identifier: NCT02923466). The

72   oncoselectivity of VSV is generally based on the type I interferon (IFN) associated antiviral

73   potential of target cells. Although VSV cannot distinguish non-malignant (herein called

74   "normal") cells from cancer cells based on their receptor profile or cell cycle, there is a big

75   difference between normal and cancer cells in their abilities to sense and respond to viral

76   infection (7). When normal cells are infected with VSV, viral infection is sensed by normal

77   cells and production of type I IFNs is triggered to impede viral replication and spread via the

78   induction of an antiviral state in the infected cells as well as the non-infected tissue

79   surrounding the IFN-producing cells. In contrast, a majority of tumors have inhibited or

80   defective type I IFN signaling (8-11), likely because many IFN responses are anti-

81   proliferative, anti-angiogenic, and pro-apoptotic (12). As VSV is highly sensitive to type I IFN

82   responses, it therefore preferentially replicates in cancer cells. The oncoselectivity of wild-

83   type (WT) VSV is not sufficient, as it is able to inhibit type I IFN signaling through one of the

84   function of the VSV matrix (M) protein, which localizes to the nuclear envelope and inhibits

85   nucleocytoplasmic trafficking of cellular mRNAs, thus impeding antiviral gene expression not

86   only in cancer, but also normal cells (13). As a result, WT VSV exhibits intolerable toxicity,

87   most notably neurotoxicity (7). Thus, an intranasal administration of VSV in rodents can

88   result in fatal infection of the central nervous system (14), and in non-human primates an

89   intrathalamic administration results in severe neurological disease (15). To address this

90   safety issue, various recombinant VSVs have been generated with a dramatically improved

91   safety and oncoselectivity profiles (5).

92   One of the well-known features of VSV is its pantropism (7), with several ubiquitously

93   expressed cell-surface molecules, such as the low-density lipoprotein receptor (LDLR) (16),

4

94 phosphatidylserine (17-19), sialoglycolipids (20), and heparan sulfate (21) suggested to play

95 a role in VSV attachment to host cells. While such pantropism does not allow VSV to

96 distinguish normal cells from cancer cells based on their differential receptor expression

97 profiles, the relative independence of VSV on a single receptor can be an advantage

98 allowing VSV-based OVs to target a wide range of tumor types. In contrast, other OVs could

99 be limited by the expression of their receptor, such as the coxsackievirus and adenovirus

100 receptor required for efficient entry of widely used adenovirus 5 based OVs (22).

101 This study focuses on pancreatic ductal adenocarcinoma (PDAC), which comprise

102 approximately 95% of pancreatic cancers. Standard cancer therapies show little efficacy in

103 treating PDAC (23) , and PDAC is expected to become the second leading cause of cancer-

104 related deaths in the U.S. by 2030 (24). Different OVs have been tested against PDAC *in*

105 *vitro* and *in vivo* with various efficacies (25). Our recent studies demonstrated that VSV is

106 effective against the majority of human PDAC cell lines, both *in vitro* and *in vivo* (26).

107 However, some PDAC cell lines are highly resistant to VSV infection, at least in part due to

108 their upregulated type I IFN signaling and constitutive expression of a subset of interferon

109 simulated genes (ISGs) (26-29). We have shown that the treatment of the resistant PDAC

110 cell lines with type I interferon inhibitors, such as JAK Inhibitor I (a pan-JAK inhibitor) or

111 ruxolitinib (a specific JAK1/2 inhibitor), significantly improve permissiveness of the cells to

112 VSV (27-29). However, this approach only moderately improved susceptibility of resistant

113 cells to VSV initial infection, and overall VSV replication never reached the level of VSV-

114 permissive PDAC cell lines (27-29). In agreement with this observation, pre-treatment of

115 cells with ruxolitinib (compared to post-treatment only) did not change the kinetics of VSV

116 replication, with a significant increase in VSV replication that could be seen only 48 hours

117 (h) post infection (p.i) even in cells pretreated with ruxolitinib for up to 48 h, suggesting that

118 ruxolitinib did not improve the rate of initial infection but rather facilitated secondary infection

119 via inhibition of antiviral signaling in PDAC cells (28, 29).

120 Together, our previous studies suggest that resistant PDAC cell lines may have an

121 additional block at an early stage of VSV infection that could not be removed via JAK

122 inhibition. In this study, we examine the role of VSV attachment in resistance of PDAC cells

123 to VSV, as it is the first critical stage for a successful VSV infection. We show that inefficient

124 VSV attachment can contribute to resistance of PDACs to VSV. Moreover, we successfully

125 used a novel approach to break the multiple mechanisms of resistance of PDAC cells to

126 VSV by combining the virus with polycations and ruxolitinib to simultaneously improve VSV

127 attachment and virus replication.

128

129 **RESULTS**

130 **VSV attachment to HPAF-II cells is impaired**

131 The human PDAC cell line HPAF-II, which showed the highest level of resistance to VSV in

132 our previous studies, was the main focus of this study (26-30). In addition, many

133 experiments included Hs766T, another VSV-resistant human PDAC cell line, as well as two

134 VSV-permissive human PDAC cell lines, MIA PaCa-2 and Suit2. This work focuses on one

135 of the most commonly used VSV-based oncolytic recombinants, VSV-ΔM51 (herein called

136 VSV; Figure legends and Materials and Methods indicate specific VSV recombinant used in

137 each experiment), which has a deletion of a methionine at position 51 in the matrix (M)

138 protein (31). This mutation causes ablation of wild type (WT) M protein's ability to inhibit

139 cellular antiviral gene expression. As many cancers have defective type I interferon antiviral

140 signaling, VSV-ΔM51 can still replicate in and kill cancer cells (32, 33). In addition, to

141 facilitate visualization of viral infection, VSV recombinants used in this study encode either

142 the near-infrared RFP (34) or GFP (31) ORF inserted between the VSV G and L genes.

143 We used two different approaches to examine the efficacy of VSV attachment to PDAC

144 cells. For fluorescence-activated cell sorting (FACS) analysis, virus attachment was

145 examined using cells in suspension (Fig. 1A). Adherent cells were treated with EDTA to

146 detach them from plastic surfaces, incubated with different amounts of VSV (MOI 1.25 or

147 12.5 based on VSV titer on MIA PaCa-2 cells) for 1 h at 4°C, washed to remove any

148 unbound virus, and analyzed for cell-bound VSV using VSV-G antibody and FACS analysis.

149 EDTA, rather than trypsin, was used to retain protein receptors of VSV (such as LDLR) on

150 the cell surface. We also assayed VSV attachment using an alternative approach, where

151 VSV attachment to cell monolayers was examined. Cells were incubated with different

152 amounts of VSV (MOI 0.1 to 250 based on MIA PaCa-2) for 1 h at 4°C, then washed to

153 remove any unbound virus, and analyzed for cell-bound VSV using western blot analysis of

154 the total cell lysates (Fig. 1B). As our study focuses on attachment, in both approaches

155 virus-cell incubations were conducted at 4°C to prevent virus entry. To confirm that VSV did

156 not penetrate cells under these conditions, cells were incubated with VSV for 1 h at 4°C,

157 trypsinized to remove all surface proteins, and analyzed for the presence of VSV. As

158 expected, no VSV products could be detected after trypsinization, indicating that VSV was

159 only bound to the cell surface (data not shown).

160 As shown in Fig. 1A for VSV attachment to cells in suspension, the lowest level of VSV

161 attachment [percentage of VSV-positive cells as well as the mean fluorescent intensity

162 (MFI)] was observed in HPAF-II under both tested conditions (MOIs). For example, at MOI

163 12.5, only 10% of HPAF-II were VSV-positive, compared to 57.4% of Hs766T, 31.9% of MIA

164 PaCa-2 and 46.5% of Suit2. In agreement with these data, we also observed lower VSV

165 attachment to HPAF-II cell monolayers (Fig. 1B, "Attachment"). Based on the serial dilutions

166 of virus and comparing VSV protein bands of similar intensity for each cell line, VSV was

167 attaching to HPAF-II cells at least 12-fold less efficiently than to MIA PaCa-2 and Hs766T

168 cells, and 3.5-fold less efficiently compared to Suit2 cells (Fig. 1B, "Attachment"). While

169 examining VSV attachment to cell monolayers, a duplicate set of samples was incubated for

170 an extra 8 h at 37°C to determine relative VSV replication levels and confirm the status of

171 PDAC cell lines in regard to their resistance/permissiveness to VSV. As shown in Fig. 1B

172 ("Replication"), MIA PaCa-2 and Suit2 are highly permissive to VSV, illustrated by high

173 levels of VSV replication at 8 h p.i., and that HPAF-II and Hs766T are resistant, with HPAF-

174 II showing the highest level of resistance (Fig. 1B, "Replication"). This result is in agreement

175 with our previous studies demonstrating that VSV-resistant PDAC cells lines (such as

176 HPAF-II and Hs766T) have upregulated type I IFN signaling and constitutive expression of a

177 subset of ISGs, whereas VSV-permissive PDAC cells lines (such as MIA PaCa-2 and Suit2)

178 do not (26-29). Interestingly, even though Hs766T had a similar level of VSV attachment as

179 MIA PaCa-2 and even higher level than Suit2 (about 3.5-fold higher based on serial dilution

180 of virus in Fig. 1B), Hs766T showed dramatically lower levels of VSV replication, compared

181 to both MIA PaCa-2 and Suit2. This result suggests that Hs766T is not defective in VSV

182 attachment. In contrast, HPAF-II showed not only the lowest levels of VSV replication, but

183 also the lowest levels of VSV attachment, suggesting that the impaired VSV attachment

184 contributes to the resistance of HPAF-II to VSV.

185

186 **LDLR expression and LDL uptake are lower in HPAF-II cells**

187 Recently, LDLR has been proposed as one of the receptors for VSV (35-37). As a high

188 variation in LDLR expression was shown between different cell lines of pancreatic origin

189 (38), we hypothesized that HPAF-II could have a defect in LDLR expression, which could

190 explain ineffective VSV attachment.

191 Three different approaches, ELISA, western blot, and FACS analysis were used to

192 determine relative levels of LDLR expression in the four PDAC cell lines. First, using an

193 LDLR ELISA assay, cell lysates were examined for cell-associated total LDLR levels in

194 PDAC cell lines. As shown in Fig. 2A, although all four tested cell lines showed detectable

195 levels of LDLR, the lowest level was in HPAF-II cells, with somewhat higher levels in MIA

196 PaCa-2 and Suit2, and the highest level in Hs766T. When cell lysates were analyzed by

197 western blot, Hs766T also showed the highest levels of LDLR (Fig. 2B). Interestingly,

198 although this analysis showed similar levels of LDLR in HPAF-II, MIA PaCa-2, and Suit2

199 cells, HPAF-II was the only cell line with an extra band underneath the main LDLR band

200 (Fig. 2B). This band generally represents an unglycosylated inactive form of LDLR, and is

201 often indicative of an abnormal LDLR processing in the cells (39-41). Because only cell

202 surface LDLR could be utilized by virus for attachment, LDLR cell surface expression was

203 examined by FACS analysis using a primary antibody against LDLR. Again, EDTA, rather

204 than trypsin, was used to retain LDLR on the cell surface. Importantly, cells were not fixed or

205 permeabilized, and were incubated at 4°C during the entire procedure to ensure that only

206 cell surface LDLR expression is detected. As shown in Fig. 2C, although all 4 cell lines

207 expressed LDLR at the cell surface, the lowest levels [percentage of LDLR-positive cells as

208 well as the MFI] were in HPAF-II. This could be due to HPAF-II expressing the

209 unglycosylated inactive form of LDLR (Fig. 2B) that is not expressed on the cell surface (39-

210 41).

211 Next, we wanted to examine LDLR functionality, which is normally done by examining the

212 uptake of low density lipoprotein (LDL), the ligand of LDLR. Importantly, LDL has been

213 previously shown to compete with VSV for LDLR (16). Therefore, the ability of LDLR to

214 uptake LDL could be used not only to examine LDLR functionality as an LDL receptor, but

215 also as a VSV receptor. To assay for LDLR functionality, PDAC cell lines were compared for

216 their abilities to uptake an exogenous fluorescently-labeled LDL. PDAC cells were incubated

217 with DiI-LDL (3,3'-dioctadecylindocarbocyanine-LDL) for 4 h, and then analyzed for the

218 levels of the internalized LDL by FACS. As shown in Fig. 2D, LDL uptake was dramatically

219 lower [percentage of LDL-positive cells as well as the MFI] in HPAF-II compared to all other

220 tested cell lines. These data demonstrate that LDLR is dysfunctional in HPAF-II, which could

221 lead to a defect of this cell line in VSV attachment.

222

223 **PDAC cell lines express wild-type LDLR**

224 Currently, more than a thousand different types of mutations have been found in the LDLR

225 protein (42). Many damaging LDLR mutations affect LDLR total expression level,

226 maturation, surface localization and LDL uptake (42). If present, such mutations could be

227 responsible for the observed lower levels of LDLR expression, LDL uptake and/or VSV

228 attachment in HPAF-II cells. To directly examine this possibility, total RNA was isolated from

229 HPAF-II, Hs766T, MIA PaCa-2, and Suit2 cells, cDNA was synthesized, PCR-amplified by

230 five pairs of LDLR specific primers (43), and the overlapping PCR products, covering the

231 entire LDLR ORF, were sequenced. Although several silent mutations were detected, the

232 sequence analysis did not detect a single mutation affecting LDLR amino acid sequence in

233 HPAF-II or any other tested PDAC cell line (data not shown). Therefore, all tested PDAC

234 cell lines produce WT LDLR. In addition, PCR fragments were analyzed by high-resolution

235 gel electrophoresis to detect alternatively spliced variants of LDLR, exactly as this method

236 was previously described (43). We did not observe any unusual PCR products, which would

237 suggest the presence of alternatively spliced variants of LDLR in HPAF-II cells (data not

238 shown). Together, our data show that the lower LDLR expression and LDL uptake in HPAF-

239 II cells were not due to LDLR mutations.

240

241 **LDLR upregulation does not improve LDL uptake or VSV attachment in HPAF-II cells**

242 The ELISA (Fig. 2A), western blot (Fig. 2B) and FACS (Fig. 2C) analyses suggested

243 potential abnormalities in the level of LDLR expression, which could explain lower LDL

244 uptake and VSV attachment. Here, we wanted to examine whether an upregulation of LDLR

245 expression would improve LDL uptake and/or VSV attachment in HPAF-II.

246 Two different drug types were tested to increase LDLR expression levels, statins and a

247 proprotein convertase subtilisin/kexin type 9 (PCSK9) inhibitor. Statins are competitive

248 inhibitors of hydroxymethylglutaryl-CoA (HMG-CoA) reductase, which is the key rate-limiting

249 enzyme of cholesterol synthesis. Statins inhibit cholesterol synthesis in the liver and some

250 other cell types, including cancer cells (44). One consequence of the decreased cholesterol

251 production is that cells compensate for it by upregulating expression of LDLR to increase

252 cholesterol uptake from the medium (45). PCSK9 is a secretory serine protease that binds

253 surface LDLR, induces its internalization and lysosomal degradation, thus inhibiting LDLR

254 recycling to the surface (46). PCSK9 inhibitors bind to PCSK9 and increase LDLR receptor

255 cycling, thus increasing surface LDLR levels and improving LDL uptake (46). Therefore, we

256 decided to use various statins and a PCSK9 inhibitor to increase LDLR expression and test

257 whether this approach could improve LDL uptake and/or VSV attachment in HPAF-II cells.

258 To increase LDLR levels prior to VSV attachment assay, HPAF-II cells were pretreated for

259 24 h with 4 widely used FDA-approved statins, atorvastatin ("Lipitor"), rosuvastatin

260 ("Crestor"), simvastatin ("Zocor"), or fluvastatin ("Lescol"), or with a PCSK9 antagonist SBC-

261   110576 (47). Other tested conditions were cell starvation (0% FBS medium), which could

262   increase LDLR levels (48), and unlabeled LDL addition that could decrease LDLR levels

263   (49-51). After 24 h treatment, cell monolayers were incubated with VSV for 1 h at 4°C to

264   examine VSV attachment using western blotting. As shown in Figure 3A, LDLR expression

265   (including the upper mature LDLR band) was strongly improved by each of the tested

266   statins, however VSV attachment levels were not improved. SBC-110576 and addition of

267   LDL did not have an effect on LDLR expression (the upper mature LDLR band) or VSV

268   attachment. However, disappearance of the lower LDLR band can be observed after SBC-

269   110576 treatment, suggesting expected improvement in LDLR maturation (Fig. 3A).

270   Interestingly, starvation did improve VSV attachment, however this was likely not due to

271   LDLR, as LDLR level were not affected by starvation (Fig. 3A). Overall, our data

272   demonstrate that increasing LDLR expression does not improve VSV attachment in HPAF-II

273   cells, suggesting that lower LDLR expression was not a main factor determining inefficient

274   VSV attachment to HPAF-II.

275   As VSV attachment was not improved by statins, we examined if the statin-mediated

276   increase in LDLR expression could improve LDL uptake in HPAF-II. Cells were pretreated

277   for 24 hours with the same statins as in the previous experiment and then incubated with

278   LDL for 4 h and then analyzed by FACS analysis. Our data show only marginal increase in

279   LDL uptake after statin treatment (Fig 3B). As both VSV attachment and LDL uptake were

280   not improved by statins, we wanted to confirm that statins improve LDLR cell surface

281   expression. HPAF-II cells were pretreated for 24 h with the same statins as in the two

282   previous experiments (Fig. 3A and 3B) and were analyzed for surface LDLR levels using

283   EDTA-isolated suspension cells and FACS analysis or by analyzing HPAF-II monolayers

284   using immunofluorescence. Cells were not fixed or permeabilized, and were incubated at

285   4°C during the entire procedure to ensure that only cell surface LDLR expression is

286   detected. FACS data (Fig. 3C) show that all statins improved LDLR cell surface expression

287   [percentage of LDLR-positive cells as well as MFI]. Immunofluorescence data (Fig. 3D)

288   were in agreement with the FACS data and also showed an increase in LDLR cell surface

289   expression. Taken together, our data indicate that the lower level of expression is not the

290   main factor of LDLR dysfunctionality in HPAF-II cells, and that some other mechanisms are

291   responsible for inefficient LDL uptake and VSV attachment.

292

293   **Role of Type I IFN signaling in LDLR expression and secretion in PDAC cells**

294   Our previous studies demonstrated that upregulated type I IFN signaling plays an important

295   role in resistance of PDAC cell lines to VSV (26-29) and that the treatment of resistant

296   PDAC cell lines with ruxolitinib (a specific JAK1/2 inhibitor) dramatically inhibits antiviral

297   signaling and improves VSV replication in all resistant PDAC cell lines (28, 29). To examine

298   whether the observed inefficient binding of VSV to HPAF-II cells is a result of the type I IFN

299   pathway upregulation, HPAF-II and Suit2 (as a negative control) cells were pretreated with

300   ruxolitinib for 24 h before performing VSV attachment to cell monolayer assay. In agreement

301   with our previous studies (28, 29), ruxolitinib treatment downregulated IFN-stimulated gene

302   (ISG) Mx1 in HPAF-II cells (Fig. 4A). However, the treatment did not improve VSV

303   attachment (Fig. 4A). This suggests that the defect of HPAF-II in VSV attachment is type I

304   IFN independent, and that the inefficient attachment and upregulated antiviral signaling

305   independently contribute to resistance of HPAF-II to VSV. In agreement with this, another

306   resistant PDAC cell line, Hs766T, does not display a defect in VSV attachment, although it

307   has the same upregulation of type I IFN signaling as HPAF-II (26-29).

308   Previous studies have shown that soluble LDLR (sLDLR) secretion by cells can be type I

309   IFN induced, and that sLDLR can inhibit VSV infection in WISH cells (this cell line has been

13

310 recently shown to be misidentified and identical to HeLa cells) (52-54). Although this

311 mechanism cannot be responsible for inefficient attachment of VSV to HPAF-II in our

312 monolayer and suspension attachment assays (cells were washed before incubation with

313 VSV), this sLDLR-mediated inhibition of VSV attachment could happen during multi-step

314 infection of cells, where HPAF-II show very strong resistance to VSV infection and

315 replication. Also, previous studies have shown that *O*-glycosylation in the stem region of

316 LDLR is important for cell surface expression and stability of this receptor, and that the

317 absence of such *O*-glycosylation can lead to proteolytic cleavage and the release into the

318 medium of the bulk of the N-terminal extracellular domain of the receptor (55, 56).

319 Therefore, an extensive release of sLDLR into the medium could be indicative of the

320 abnormal LDLR *O*-glycosylation in HPAF-II cells.

321 First, to test whether sLDLR can inhibit VSV infectivity in PDACs, sLDLR and VSV or VSV

322 alone were added to the cells and incubated for 30 min at 37°C [the assay was conducted

323 as described previously (52-54)]. Cells were then washed to remove any unbound virus and

324 overlaid with agar to prevent secondary infections. VSV plaques were counted to determine

325 the effect of sLDLR on VSV infectivity. As shown in Fig. 4B, the presence of the exogenous

326 sLDLR led to a 10-fold decrease in VSV infectivity, confirming that sLDLR secretion could

327 potentially inhibit VSV attachment in PDAC cell lines. To examine the levels of secreted

328 sLDLR produced by different PDAC cell lines, cells were incubated for 24 h in a medium

329 without FBS, the medium then was collected and analyzed by ELISA for sLDLR. As shown

330 in Figure 4C, the tested PDAC cell lines produced different amount of sLDLR. Importantly,

331 HPAF-II did not produce the most sLDLR, possibly suggesting no abnormalities in this cell

332 line in *O*-glycosylation or other mechanisms associated with excessive secretion of sLDLR.

14

333   In addition, the effects of type I IFN on sLDLR secretion or total LDLR levels in PDAC cells

334   were examined. PDAC cell lines were treated either with IFN-α (to stimulate type I IFN

335   signaling) or ruxolitinib (to inhibit it) or both, and sLDLR (Fig. 4D) and cell-associated LDLR

336   (Fig. 4E) levels were analyzed using ELISA assay. In contrast to previous studies with

337   WISH cells (52, 53), the treatments had either no or negligible effects on sLDLR production

338   and cell-associated LDLR. Furthermore, when HPAF-II were treated with ruxolitinib (to

339   inhibit type I IFN signaling), LDL uptake was not improved (Fig. 4F). Together, our data

340   demonstrate that HPAF-II cells do not display abnormalities in sLDLR secretion levels, and

341   that LDLR expression, LDL uptake and VSV attachment in PDAC cells are controlled

342   independently of type I IFN signaling.

343

344   **Polycations improve VSV attachment to HPAF-II cells**

345   Our data show that inefficient VSV attachment to HPAF-II cells, as well as defective LDL

346   uptake, could not be improved in HPAF-II cells even when LDLR expression was markedly

347   increased by treating cells with statins (Fig. 3). While future studies are needed to identify

348   specific defects of LDLR in LDL uptake and VSV attachment, here we decided to use an

349   alternative approach to improve VSV attachment by targeting LDLR-independent VSV

350   attachment. Previous studies have suggested that phosphatidylserine (17-19),

351   sialoglycolipids (20), heparan sulfate (21), or electrostatic interactions between VSV and cell

352   membrane (57, 58) could play an important role in VSV attachment. As none of these

353   studies examined PDAC cell lines, we want to confirm that LDLR-independent attachment

354   also occurs in PDAC cell lines. Cells were treated with 0.2% EDTA (control) or 0.05%

355   trypsin in PBS for 30 min at 37°C to digest surface LDLR, then used for FACS analysis of

356   VSV attachment to cells in suspension (Fig. 5A). To confirm successful digestion of LDLR

357　　by trypsin, total protein was isolated from trypsin-treated cells and analyzed by western

358　　blotting for LDLR (Fig. 5B). Despite the lack of any detectable LDLR in trypsin-treated

359　　HPAF-II, MIA PaCa-2, and Suit2 cell lines, and a significant decrease of the mature LDLR

360　　(upper band) in Hs766T cells (Fig. 5B), VSV attachment occurred in all cell lines (Fig. 5A).

361　　Again, HPAF-II showed the lowest level of VSV attachment, as they are defective in VSV

362　　attachment even in the presence of LDLR, when the analyzed cells were detached using

363　　EDTA (Fig. 5A). These data suggest that VSV particles can attach to PDAC cells in an

364　　LDLR-independent manner.

365　　There are several approaches to improve LDLR-independent VSV attachment to cells.

366　　Several early studies demonstrated that different pH conditions or the addition of positively-

367　　charged polycations, such as polybrene or DEAE-dextran, can significantly improve VSV

368　　attachment to various cell membrane components via nonspecific electrostatic interactions

369　　(57-59). Moreover, polybrene and other polycations are routinely used to improve

370　　transduction of target cells with replication-defective lentiviral particles that are pseudotyped

371　　with VSV-G (60-62). Therefore, all these conditions were examined to identify a way to

372　　improve VSV attachment to HPAF-II cells. Our original screen was conducted under

373　　conditions most optimal for VSV attachment, and we used VSV-driven GFP expression as a

374　　readout of virus infection/replication. Any conditions stimulating VSV infection were then

375　　studied in the subsequent experiments for their specific effect on VSV attachment. To

376　　examine whether pH or polycations can improve VSV infection of HPAF-II cells, cells were

377　　pretreated for 30 min with various concentrations of protons (pH levels), polybrene or

378　　DEAE-dextran, then incubated with VSV for 1 h at 37°C in the presence of each test

379　　condition (Fig. 6A and 6B). Virus and chemical reagents then were removed and cells were

380　　placed back at 37°C for 46 h, and VSV infection driven GFP fluorescence was measured.

381　　As different pH conditions or polycations were present only for 1 h 30 min and removed after

16

382   virus incubation, the differences in VSV-associated GFP fluorescence identified in this

383   original screening were likely reflecting the efficacy of VSV initial infection. None of the pH

384   conditions improved VSV infection in HPAF-II [(Fig. 6A, each condition is compared to GFP

385   fluorescence in HPAF-II cells treated with VSV only ("VSV Control")]. However, among all

386   tested conditions, the two highest tested concentrations (10 µg/ml and 50 µg/ml) of

387   polybrene and DEAE-dextran showed a clear increase in VSV infectivity (Fig. 6A). To

388   examine whether the improved VSV infectivity under these treatment conditions results in

389   increased oncolysis, an MTT cell viability assay was performed 5 days p.i. Compared to

390   VSV alone ("VSV Control"), the 2 highest concentrations (10 and 50 µg/ml) of polybrene and

391   all 3 concentrations of DEAE-dextran significantly decreased cell viability (Figure 6B).

392   To examine whether the observed improvement in VSV infectivity was due to an

393   improvement in VSV attachment, cells in monolayer or in suspension were pretreated for 30

394   min with 10 µg/ml of polybrene or DEAE-dextran, then incubated with VSV for 1 h at 4°C (to

395   prevent virus entry) in the presence of these polycations. Cells were washed to remove any

396   unbound virus, then protein was isolated from cells in monolayer and analyzed by western

397   blotting or cells in suspension were used for FACS analysis. Both polybrene and DEAE-

398   dextran treatments did show a clear improvement in VSV attachment for both methods,

399   even though the improvement with DEAE-dextran was stronger (Fig. 6C and 6D). The

400   FACS data showed that polycations more than doubled the number of cells attached by

401   VSV (Fig 6D).

402   We then tested whether the improved VSV attachment to HPAF-II was possibly due to an

403   increased LDLR expression or functionality as a result of the treatments of cells with

404   polycations. Pretreatment of cells for 30 min with 10 µg/ml of polybrene or DEAE-dextran,

405   followed by incubation with VSV for 1 h at 4°C in the presence of these polycations did not

17

406   improve LDLR expression (Fig. 6C). Furthermore, when cells were pretreated for 30 min

407   with 10 µg/ml of polybrene or DEAE-dextran then incubated with LDL for 4 h at 37 °C in the

408   presence of these polycations, no improvement in LDL uptake was observed when cells

409   were analyzed by FACS analysis (Fig. 6E). Taken together, these data indicate that

410   polybrene and DEAE-dextran improve VSV attachment to HPAF-II cells via an LDLR-

411   independent mechanism.

412

413   **Combining polybrene or DEAE-dextran with ruxolitinib breaks resistance of PDAC**

414   **cells to VSV**

415   We have shown previously that the treatment of HPAF-II and other resistant PDAC cell lines

416   with JAK1/2 inhibitors significantly improve their permissiveness to VSV (27-29). However,

417   JAK Inhibitor I treatment only moderately improves susceptibility of resistant cells to VSV

418   initial infection (27), and pre-treatment of cells with ruxolitinib (compared to post-treatment

419   only) did not change the kinetics of VSV replication, with a significant increase in VSV

420   replication that could be seen only after 48 h p.i even in cells pretreated with ruxolitinib for

421   up to 48 h, suggesting that ruxolitinib did not improve the rate of initial infection but rather

422   facilitated secondary infection via inhibition of antiviral signaling in PDAC cells (27-29). As

423   polybrene and DEAE-dextran improve VSV attachment and primary infection and ruxolitinib

424   improves VSV replication, we hypothesized that combining these two treatments would

425   improve overall VSV infection and oncolysis in HPAF-II cells. Cells were pretreated with 10

426   µg/ml polybrene or DEAE-dextran or mock-treated for 30 min, then VSV was added in the

427   presence of polycations (or mock treatment) for 1 h at 37 °C, followed by media removal

428   and washes with PBS, and then cells were incubated in the presence of 2.5 µM ruxolitinib or

429   mock treatment. VSV infection-associated GFP fluorescence was monitored for 71 h. In

430   agreement with our previous study (28), ruxolitininb alone significantly improved VSV

431   replication starting at 48 h p.i., however the polycation/ruxolitinib combinations showed even

432   stronger improvement (Fig. 7A). Importantly, the polycation/ruxolitinib combinations did not

433   only result in higher VSV replication (Fig. 7A), but also the significant increase in VSV

434   replication was already seen at 24 h p.i. versus 48 h p.i. for ruxolitinib treatment only (Fig.

435   7A), likely due to polybrene and DEAE-dextran improving the rate of initial infections, as

436   these polycations were present only during 1 h incubation of HPAF-II cells with VSV. Figure

437   7B shows representative pictures of the treated cells at 22 and 48 h p.i., and it confirms that

438   an important improvement in VSV replication can already be seen at 22 h p.i. for the

439   polycation/ruxolitinib combinations. To examine whether the improved VSV infectivity under

440   these treatment conditions results in increased oncolysis, an MTT cell viability assay was

441   performed 71 h p.i. Ruxolitinib did improve oncolysis significantly, however the

442   polycation/ruxolitinib combination significantly improved oncolysis compared to ruxolitinib

443   alone treatment (Fig. 7C).

444   To confirm that polybrene and DEAE-dextran improve initial infections, HPAF-II cells were

445   treated as in the previous experiment, however cells were analyzed by FACS for the

446   number of infected cells at an earlier time point (18 h p.i.), when for HPAF-II we generally

447   observe only initially infected cells (Figure 8D). Polybrene and DEAE-dextran treatments

448   resulted in many more GFP-positive cells (55.7% and 55.9%, respectively, versus 1.1% for

449   VSV only) than the ruxolitinib condition (27%), confirming that these polycations improved

450   initial infection. When the polycations were combined with ruxolitinib, almost all cells were

451   infected (90.3% and 83.6% for polybrene/ruxolitinib and DEAE-dextran /ruxolitinib,

452   respectively), likely because the initial infections were improved by polybrene or DEAE-

453   dextran, and secondary infections were improved by ruxolitinib via enhancement of VSV

454   replication in the initially infected cells and inhibition of antiviral responses in the secondary-

19

455   infected cells. Taken together, polycations and ruxolitinib complement each other when

456   combined and break the multiple mechanisms of resistance of HPAF-II to VSV.

457   To evaluate if the combination treatment could work on a broad spectrum of PDAC cell

458   lines, Hs766T, MiaPaCa-2 and Suit2 were treated as HPAF-II previously (Fig. 7A and 7B).

459   The VSV-resistant PDAC cell line Hs766T and VSV-permissive cell line Suit2 responded

460   similarly to HPAF-II as the combination treatment resulted in higher VSV replication and a

461   significant increase in VSV replication was already seen at 22 h p.i. versus 46 h p.i. for

462   ruxolitinib treatment only (Fig. 8). The VSV-permissive cell line MiaPaCa-2 also resulted in a

463   somewhat higher VSV replication, however a smaller increase was seen at 22 h p.i. when

464   compared to ruxolitinib alone (Fig. 8). This is not surprising as MiaPaCa-2 is the most

465   permissive PDAC cell line and, based on our previous studies, it has the strongest defect in

466   antiviral signaling (26-29). To examine whether the improved VSV infectivity under these

467   treatment conditions results in increased oncolysis, an MTT cell viability assay was

468   performed 68 h p.i. Oncolysis of the VSV-resistant PDAC cell line Hs766T was significantly

469   improved by ruxolitinib, however the polycation/ruxolitinib combination significantly improved

470   oncolysis compared to ruxolitinib (Fig. 8). With VSV-mediated oncolysis being already very

471   efficient in VSV-permissive PDAC cell lines, the polycation/ruxolitinib combination did not

472   improve oncolysis (Fig. 8). Taken together, polycations and ruxolitinib can improve VSV

473   treatment outcome in a wide spectrum of PDAC cell lines.

474

475   **DISCUSSION**

476   In this study, we examined a possible role of virus attachment in the resistance of some

477   human PDAC cell lines to VSV, as it is the first critical stage for a successful viral infection.

478   We demonstrate that HPAF-II, the most resistant PDAC cell line, in addition to an

479   upregulated type I IFN signaling and a constitutive expression of ISGs, also shows impaired

480   VSV attachment. This result was surprising as VSV is known for its pantropism and the

481   ability to infect virtually any cell line (of vertebrate or invertebrate origin) in the lab (7).

482   Importantly, pretreating HPAF-II cells with ruxolitinib did not improve VSV attachment

483   indicating that type I IFN signaling does not play a major role in VSV attachment. In general,

484   our results suggest that HPAF-II cells are highly resistant to VSV because they are not only

485   non-permissive to VSV replication due to their constitutive antiviral state, but also non-

486   susceptible to VSV due to impaired virus attachment, which is type I IFN independent.

487   As LDLR has been shown to be one of the receptors for VSV (35-37), our study examined if

488   HPAF-II cells have a defect in LDLR expression or functionality. Our data show that HPAF-II

489   has lower LDLR expression. Moreover, based on the LDL uptake assay, HPAF-II cells

490   express dysfunctional LDLR, which could explain the defect of this cell line in VSV

491   attachment. More than a thousand different types of mutations have been found in the

492   LDLR protein, which affect LDLR expression or functionality (42). With mutations being so

493   common in LDLR, we hypothesized that HPAF-II could have a mutation in LDLR, which

494   would explain its defects in LDL uptake and VSV attachment. However, our sequence

495   analysis of LDLR mRNA showed no mutations affecting LDLR amino acid sequence in

496   HPAF-II (or other 3 tested PDAC cell lines), suggesting that other factor(s) are responsible

497   for lower expression and/or activities of LDLR in HPAF-II cells. To improve the LDLR

498   expression and LDL uptake, HPAF-II were treated with statins. Although all four tested

499   statins strongly increased total and surface LDLR expression, this increase did not improve

500   LDL uptake and VSV attachment in HPAF-II.

501   Taken together, the defective uptake of LDL and impaired VSV attachment in HPAF-II were

502   not determined by mutations or a relatively lower LDLR expression levels in this cell line, but

21

503   via some other mechanism(s). Previous studies have shown that *O*-glycosylation in the

504   stem region of LDLR is important for cell surface expression and stability of this receptor.

505   Absence of *O*-glycosylation in the stem region can lead to proteolytic cleavage and the

506   release into the medium of the bulk of the N-terminal extracellular domain of the receptor

507   (55, 56). It is possible that HPAF-II is lacking *O*-glycosylation, however it is important to note

508   that HPAF-II did not release the most sLDLR into the medium, compared to other tested

509   PDAC cells, which express functional LDLR. It has also been suggested that the N-terminal

510   segment of LDLR also has *O*-glycans (63). Although the same study demonstrated that *O*-

511   glycosylation at the N-terminal segment of LDLR did not affect LDLR cell surface expression

512   and LDL binding/internalization (63), another group has shown in another cell line that N-

513   terminal *O*-glycosylation is important for LDLR function as it showed an effect on LDL

514   binding (64).

515   It is also possible that HPAF-II cells express normal levels of functional LDLR, but a

516   negative factor on the cell surface of HPAF-II interferes with LDL uptake and VSV

517   attachment, and even with LDLR antibody binding in our FACS assay. Interestingly, MUC1

518   mucin overexpression in some PDAC cell lines, including HPAF-II, have been shown to limit

519   the uptake of anticancer drugs by tumor cells (65, 66). It is possible that MUC1 and other

520   mucins masks LDLR and prevents both VSV attachment and LDL uptake. Future studies

521   will examine all these possibilities.

522   As statin-mediated increase in LDLR expression did not improve VSV attachment or LDLR

523   functionality, we evaluated LDLR independent mechanisms to improve VSV attachment.

524   While LDLR is suggested as one of the receptors for VSV (35), previous studies have also

525   suggested that phosphatidylserine (17-19), sialoglycolipids (20), heparan sulfate (21) and

526   virus/cell membrane electrostatic interactions (57, 58) may play an important role in VSV

22

527 attachment. We employed a cell surface "shaving" technique with trypsin to remove surface

528 LDLR, and our data showed that VSV can indeed attach to PDAC cells in an LDLR-

529 independent VSV manner. We then decided to test two commonly used polycations,

530 polybrene or DEAE-dextran, which previously have shown to improve VSV attachment (57,

531 58), and also used in various application using VSV-G pseudotyped lentiviruses (60-62).

532 Adding these polycations strongly improved VSV attachment, VSV infection and VSV

533 induced cell death. These improvements in VSV attachment were LDLR independent as the

534 polycations had no effect on LDL uptake or LDLR expression.

535 As the cell and virus lipid membrane both possess net-negative charges, it is suggested that

536 polycations act by counteracting repulsive electrostatic effects and thus improving

537 attachment. Early studies have shown that treatment of HeLa cells with polybrene has to be

538 done before the infection and/or during the infection but not after the infection with VSV (57,

539 59). The study concluded that polybrene must have an effect on VSV binding to cells

540 potentially by improving virus/receptor interaction. Studies on DEAE-dextran made similar

541 observations and concluded that alterations in cell surface charge distribution enhance VSV

542 attachment (57, 58). More recent studies using retroviruses observed that polybrene

543 increased their attachment by 10-fold (67). Interestingly, this enhancement was receptor

544 and virus envelope independent, as retrovirus adsorption occurred equivalently on receptor

545 positive and negative cells, as well as with envelope positive and negative ("bald") virus

546 particles. The study concluded that electrostatic interactions play an important role in

547 mediating early virus-cell interactions (67).

548 Our data not only show that polycations strongly improve VSV attachment to HPAF-II cells,

549 but we also successfully used a novel triple combination treatment to break multiple

550 mechanisms of resistance of HPAF-II cells to VSV. We have previously shown that adding

551 pre-treatment of cells with ruxolitinib (compared to post-treatment only) did not change the

552 kinetics of VSV replication, suggesting that ruxolitinib had a modest effect on the initial

553 infection but mainly facilitated secondary infection via inhibition of antiviral signaling in

554 PDAC cells (28, 29). Here, combining polycations (improving initial infection) with ruxolitinib

555 (improving viral replication) did not only improve overall VSV replication and oncolysis but

556 also accelerated VSV replication kinetics by 24 h, compared to ruxolitinib only treatment

557 (Fig. 9).

558 The primary goal of this study was to determine if VSV attachment could be a limiting factor

559 in VSV-based oncolytic virotherapy against PDAC. We demonstrated that VSV attaches

560 significantly less to most resistant PDAC cell line HPAF-II, and this mechanism contributes

561 to the resistance of HPAF-II to VSV infection. Also, for the first time, we show that

562 combining a polycation with a JAK inhibitor can improve the outcome of oncolytic virus

563 treatment *in vitro*. Future experiments will test at least some of these combinations *in vivo* in

564 a clinically-relevant PDAC animal model. Previous studies examining polycations were done

565 in the context of gene therapy to improve viral as well as non-viral gene delivery (68), as

566 inefficient gene delivery is often a major limitation in the success of gene therapy (69). The

567 effects of polycations *in vitro* and *in vivo* have been extensively studied for adenovirus-

568 based gene therapy vectors. Several studies in different mouse models have shown that

569 combining adenovirus with different polycations (including DEAE-dextran) can improve

570 adenovirus-mediated gene transfer without any additional toxicity (70-73). As polycations

571 improve adenovirus-mediated gene transfer, less virus would have to be used, which would

572 improve the therapeutic index by reducing unwanted responses associated with high doses

573 of virus. On the other hand, multiple reports indicate that polycations could exhibit

574 nonspecific cytotoxicity *in vivo* as well as *in vitro* (74, 75), with some studies demonstrating

575 unacceptable cytotoxicity for DEAE-dextran (75, 76) and polybrene (77, 78), at least under

24

576   some experimental conditions. Therefore, while our study conceptually demonstrates the

577   feasibility of the polycation-mediated improvement of VSV-based OV therapy *in vitro*, future

578   studies are needed to compare polybrene and DEAE-dextran to other polycations that could

579   be used safely and effectively *in vivo* in combination with VSV and ruxolitinib. For instance,

580   the non-specific cytotoxicity of polycations is already being addressed currently through

581   development of biodegradable polycations (79). We envision that polycations would be

582   particularly useful during initial infection, especially in context of intratumoral injection, in

583   maximizing the number of initially infected cells, while ruxolitinib would stimulate replication

584   and spread of the virus within tumors.

585   In regard to ruxolitinib, this drug was recently approved by the FDA for the treatment of

586   patients with intermediate or high-risk myelofibrosis (80). It is important to be aware that

587   inhibition of innate antiviral responses by ruxolitinib or other inhibitors of antiviral response

588   could potentially result in increase of VSV virulence in normal tissues. However, it has

589   recently been shown that ruxolitinib enhanced VSV oncolytic virus treatment *in vivo*, both in

590   subcutaneous as well as orthotopic xenograft mouse models of ovarian cancer, without

591   causing significant additional toxicity (81). Moreover, other combined treatments of VSV with

592   inhibitors of antiviral responses were examined *in vivo* and also were shown to be effective

593   and safe. For example, VSV in combination with rapamycin, the inhibitor of mammalian

594   target of rapamycin (mTOR, stimulates type I IFN production via phosphorylation of its

595   effectors) selectively killed tumor, but not normal cells and increased the survival of

596   immunocompetent rats bearing malignant gliomas. In addition, histone deacetylase (HDAC)

597   inhibitors MS-275 or SAHA reversibly compromised host antiviral responses and enhanced

598   spread of VSV in various cancer types, with no detection of VSV in normal tissues (82-84).

599   Our future *in vivo* experiments will address the efficacy and safety of the triple combination

600   treatment of VSV with ruxolitinib and a polycation. To fully examine the anticancer abilities

601 and safety of this treatment, it will need to be tested in an immunocompetent *in vivo* system.

602 Unfortunately, our current *in vitro* system, based on clinically-relevant human PDAC,

603 complicates this task, as HPAF-II and other human PDAC cell lines cannot be tested in

604 immunocompetent mice. Also, in our previous study all tested mouse PDAC cell lines had

605 defective type I IFN signaling and were highly permissive to VSV (85). Currently, we are

606 examining several other mouse PDAC cell lines for their type I IFN status and

607 susceptibility/permissiveness to VSV. Based on this study, we expect to identify VSV-

608 permissive and VSV-resistant mouse PDAC cells lines that could be tested with

609 VSV/ruxolitinib/polycation combinations in immunocompetent mouse model of PDAC. We

610 envision that this novel triple combination (VSV/ruxolitinib/polycation) approach could be

611 used in the future to treat PDAC tumors highly resistant to OV therapy.

612

613 **MATERIALS AND METHODS**

614 **Viruses and cell lines.** The recombinant VSV-ΔM51-eqFP650 (34) or VSV-ΔM51-GFP (31)

615 have been described previously. VSV-ΔM51 has a deletion of the methionine at amino acid

616 position 51 of the matrix protein. In addition, VSV-ΔM51-eqFP650 has the near-infrared

617 fluorescent protein open reading frame (ORF) (34) and VSV-ΔM51-GFP has the green

618 fluorescent protein (GFP) ORF (31) inserted between the VSV G and L genes. For

619 attachment assay, viruses were ultra-purified exactly as previously described (86). The

620 following human PDAC cell lines were used in this study: HPAF-II (ATCC CRL-1997),

621 Hs766T (ATCC HTB-134), MIA PaCa-2 (ATCC CRL-1420), and Suit2 (87). The human

622 origin of all these PDAC cell lines was confirmed by partial sequencing of KRAS and actin.

623 As expected, all PDAC cell lines had a mutation in KRAS, as is typical for PDACs (28, 29).

624 The baby hamster kidney BHK-21 fibroblast cell line (ATCC CCL-10) was used to grow

625   viruses and determine their titers. MIA PaCa-2, Hs766T, and Suit2 cells were maintained in

626   Dulbecco's modified Eagle's medium (DMEM, Cellgro, 10-013-CV), while HPAF-II and BHK-

627   21 in modified Eagle's medium (MEM, Cellgro, 10-010-CV). All cell growth media were

628   supplemented with 9% fetal bovine serum (FBS, Gibco), 3.4 mM L-glutamine, 900 U/ml

629   penicillin and 900 μg/ml streptomycin (HyClone). MEM was additionally supplemented with

630   0.3% glucose (w/v). Cells were kept in a 5% CO_2 atmosphere at 37°C. For all experiments,

631   PDAC cell lines were passaged no more than 15 times.

632

633   **VSV attachment assay.** VSV-ΔM51-eqFP650 was used for all attachment assays. To

634   assay for VSV attachment to cells in suspension, adherent cells were washed one time with

635   PBS and then treated with PBS with 0.2% EDTA or 0.05% trypsin for 30 minutes (min) to

636   detach them from the surface. DMEM or MEM with 10% FBS was then added for trypsin

637   neutralization, and cells then were washed one time with PBS. Cells were then

638   resuspended in DMEM or MEM (without FBS) and incubated for 1 h at 4 °C (the rest of the

639   procedure is done at 4 °C) for VSV attachment. After the incubation, cells were washed 3

640   times with PBS to remove any unbound virus. Cells were resuspended in PBS with 2% BSA

641   and blocked for 10 min, followed by a 1 h incubation with 1:1000 VSV-G antibody [Kerafast,

642   8G5F11] and a 30 min incubation with 1:10 Mouse F(ab)2 IgG (H+L) APC-conjugated

643   antibody (R&D, F0101B). Cells were analyzed using the LSR Fortessa cell analyser (BD

644   Bioscience), and the data were analyzed to determine the percentage of positive cells and

645   the mean fluorescent intensity (MFI) with FlowJo software (Treestar). MFI represents the

646   arithmetic mean, so the average fluorescent intensity of cells in the population displayed on

647   the histogram. To assay for VSV attachment to the cell monolayer, cells were seeded in a 6-

648   well or 12-well plate such that confluency was at 80% the next day. Media was then

27

649 removed, and cells were washed one time with PBS. Virus in DMEM or MEM (without FBS)

650 then was added, and cells were incubated on a rocker for 1 h at 4°C. After incubation, wells

651 were washed 3 times with PBS to remove any unbound virus. Protein isolation buffer was

652 added and western blot analysis was performed (as described below).

653

654 **Protein Isolation and western blot analysis.** Cells were seeded in a 6-well or 12-well

655 plate and treated as described above. Media was removed and cells were lysed in non-

656 reducing conditions with lysis buffer containing 0.0625 M Tris-HCl (pH 6.8), 10% glycerol,

657 2% SDS and 0.02% (w/v) bromophenol blue. We used the non-reducing conditions, as

658 reduction of disulfide bridges in the LDLR from the medium has been reported to prevent

659 the binding of both LDL and the well-characterized LDLR antibodies (88-90). Total protein

660 was separated by electrophoresis on SDS-PAGE gels and electroblotted to polyvinylidene

661 difluoride membranes. Membranes were blocked using 5% non-fat powdered milk in TBS-T

662 [0.5 M NaCl, 20 mM Tris (pH 7.5), 0.1% Tween20]. Membranes were incubated with 1:5000

663 rabbit polyclonal anti-VSV antibodies (raised against VSV virions), 1:2000 anti-LDLR (R&D

664 Systems, AF2148) or 1:1000 anti-MX1 (Sigma-Aldrich, 631-645) in TBS-T with 5% BSA or

665 5% milk with 0.02% sodium azide. The goat anti-mouse or goat anti-rabbit or chicken anti-

666 goat horseradish peroxidase-conjugated secondary antibodies (Jackson-ImmunoResearch)

667 were used. The Amersham ECL Western Blotting Detection Kit (GE Healthcare) was used

668 for detection. To verify total protein in each loaded sample, membranes were re-probed with

669 rabbit 1:1000 anti-GAPDH antibody (Santa Cruz, sc-25778) or stained with Coomassie blue

670 R-250.

671

672   **ELISA.** Cells were seeded in a 96-well plate with appropriate media (9% FBS) so that they

673   were 80% confluent the next day. The wells were then aspirated, washed one time with

674   PBS and replaced with appropriate media (0% FBS) and treatment. The treatments

675   consisted of DMSO only, IFN (Calbiochem 407294-5MU) (5000 U/ml), ruxolitinib

676   (INCB018424, trade names Jakafi and Jakavi) (2.5 μM) and IFN (5000 U/ml) / ruxolitinib

677   (2.5 μM) mixture in appropriate media with 0% FBS. All conditions contained 0.1% DMSO.

678   Cell culture lysates and supernates were isolated 24 h later and analyzed by ELISA for

679   cellular LDLR and soluble LDLR (sLDLR), respectively, according to manufacturer's

680   instructions (Human LDL R Quantikine ELISA kit, R&D Systems, DLDLR0).

681

682   **Fluorescence-activated cell sorting (FACS) analysis of LDLR cell surface expression.**

683   For the LDLR cell surface expression experiment, cells were washed one time with PBS and

684   then incubated with 0.2% EDTA in PBS (to retain LDLR on the cell surface). When the

685   adherent cells detached, cells were counted with hemocytometer, and 1 million cells were

686   used per condition. Three conditions were used for each cell line: cells alone, cells with

687   secondary antibody (indicated as "control" in the figures) and cells with primary and

688   secondary antibody (indicated as "LDLR" in the figures). Cells were not fixed or

689   permeabilized, and were incubated at 4°C during the entire procedure. Cells were first

690   blocked in 2% BSA for 10 min, then incubated with 1:10 primary antibody against human

691   LDLR (R&D Systems, AF2148) for 30 min and then incubated with 1:10 secondary antibody

692   (Goat IgG (H+L) APC-conjugated antibody; R&D Systems, F0108) for 15 min. Cells were

693   washed with PBS one time after incubation with the primary antibody and six times after

694   secondary antibody. Cells were analyzed on a LSR Fortessa cell analyser (BD Bioscience),

695   and the data were analyzed with FlowJo software (Treestar).

29

696

LDL uptake assay. For the LDL uptake assay, cells were seeded in 6-well plates. Media

was then aspirated, wells were washed one time with PBS, and then DMEM or MEM with

0% FBS was added. Fluorescently labeled LDL from human plasma (Molecular Probes,

L3482) was then added at the concentration of 3 µg/ml to the media for 4 h at 37°C. Media

was then aspirated and cells were washed 3 times with PBS to remove unbound LDL. Cells

were then incubated with 0.05% trypsin in PBS to eliminate LDL that bound but did not enter

into the cells. Cells were analyzed using the LSR Fortessa cell analyser (BD Bioscience),

and the data were analyzed with FlowJo software (Treestar).

705

Immunofluorescence. For the LDLR cell surface expression analysis, cells were seeded in

24-well plates. Cells were not fixed or permeabilized, and were incubated at 4°C during the

entire procedure. Cells were washed two times with PBS, blocked in 5% BSA for 30 min,

then incubated with 1:20 primary antibody against human LDLR (R&D Systems, AF2148)

for 1 h and then incubated with 1:200 secondary antibody (Rabbit anti-Goat IgG (H+L)

Cross-Adsorbed Secondary Antibody, Alexa Fluor 488; Thermo Fisher, A-11078) for 1 h.

Cells were washed with PBS three times after incubation with the primary antibody and after

secondary antibody. Cell were visualized with Olympus IX70 and pictures were taken with

AxioCam HRc Zeiss.

715

VSV infection inhibition by soluble LDLR. To analyze the effect of soluble sLDLR on VSV

infectivity, cells were seeded in 12-well plates so that they were 80% confluent the next day.

Media was then aspirated, wells were washed one time with PBS and then DMEM with 0%

719   FBS was added. First, sLDLR (R&D Systems, 2148-LD-025) was added at a concentration

720   of 1 µg/ml and then VSV-ΔM51-eqFP650 was added. Cells were incubated with the mixture

721   for 30 min at 37°C. Then cells were washed 3 times with PBS, and overlaid with 0.5% agar

722   containing DMEM (5% FBS). Plaques were counted 16 h later to determine titer.

723

724   **Effect of statins on VSV attachment, LDL uptake and LDLR cell surface expression.**

725   Atorvastatin Calcium (S2077), Fluvastatin Sodium (S1909), Rosuvastatin Calcium (S2169),

726   Simvastatin (S1792) and SBC-115076 (S7976, a PCSK9 antagonist) were purchased from

727   Selleck Chemicals. Cells were seeded so that they were 80% (VSV attachment and LDL

728   uptake) or 50% (LDLR cell surface expression) confluent the next day. Media was then

729   aspirated, washed one time with PBS and then statins or a SBC-115076 were added at

730   appropriate concentration in MEM with 5% FBS for 24 hours. VSV attachment (monolayer),

731   LDL uptake or LDLR cell surface expression (FACS and immunofluorescence) assays were

732   performed as described above.

733

734   **Effect of polycations on VSV infectivity, cell viability and VSV attachment.** HPAF-II

735   cells were seeded in a 96-well plate such that they were approximately 90% confluent at the

736   time of treatment. Cells were washed once with PBS. For each test condition, various

737   concentrations of DEAE-dextran (Alfa Aesar J63781) or polybrene (Millipore TR-1003-G)

738   and protons in MEM without FBS were added to cells. For control wells, MEM without FBS

739   was added. The plate was incubated at 37°C for 30 min during which it was rocked every 5

740   min. VSV-ΔM51-GFP in MEM without FBS at MOI 0.1 based on HPAF-II cells was added

741   and incubated for 1 h with rocking every 10 min. The mixture was aspirated, wells washed 3

742   times with PBS, MEM with 5% FBS was added to wells, and cells were incubated at 37°C.

743   GFP fluorescence was measured at regular intervals (CytoFluor Series 4000, excitation filter

744   of 485/20 nm, emission 530/25 nm, gain=63; Applied Biosystems). 5 days post infection,

745   cell viability was determined by methylthiazolydiphenyl-tetrazolium (MTT) cell viability assay

746   (Biotium). For VSV attachment in monolayer, HPAF-II cells were seeded in a 12-well plate

747   such that they were approximately 80% confluent at the time of treatment. Polybrene and

748   DEAE-dextran, both at 10 μg/mL in MEM without FBS, were incubated with cells for 30 min

749   at 4°C. Cells were then incubated with VSV-ΔM51-eqFP650 at MOI 250 based on MIA

750   PaCa-2 for 1 h at 4°C. Then VSV attachment assay to monolayer was followed as

751   described above. For VSV attachment in suspension, HPAF-II cells were seeded in a T75

752   flask such that they were approximately 90% confluent at the time of treatment. Cells were

753   washed once with PBS. The flask was incubated for 30 min after the addition of 0.05%

754   trypsin for cell detachment. MEM with 10% FBS was added to neutralize trypsin. Cells were

755   kept at 4°C during cell counting. HPAF-II cells were split into one million cell portions and

756   transferred to 1.5 mL tubes. Polybrene and DEAE-dextran, both at 10 μg/mL in MEM

757   without FBS, were incubated with cells for 30 min with 5 min between mixes at 4°C. Cells

758   were then incubated with VSV at MOI 125 based on MIA PaCa-2 for 1 h at 4°C with 15 min

759   between inversions. Then VSV attachment assay to cells in suspension was followed as

760   described above. For LDL uptake, HPAF-II cells were seeded in a 6-well plate such that

761   they were approximately 80% confluent at the time of treatment. Polybrene and DEAE-

762   dextran, both at 10 μg/mL in MEM without FBS, were incubated with cells for 30 min at 4°C.

763   Cells were then incubated with fluorescently labeled LDL from human plasma (Molecular

764   Probes, L3482) at the concentration of 3 μg/ml to the media in the presence of polycations

765   for 4 h at 37°C. The LDL uptake protocol was then followed as described above.

766

Effects of combination of polycations and ruxolitinib on VSV infectivity, replication and cell viability. HPAF-II, Hs766T, MIA PaCa-2 and Suit-2 cells were seeded in a 96-well plate such that they were approximately 80% confluent at the time of treatment. Cells were washed once with PBS. For each test condition, polybrene or DEAE-dextran in MEM without FBS was added to cells at a concentration of 10 μg/mL. For control and ruxolitinib wells, MEM without FBS was added. The plate was incubated at 37°C for 30 min during which it was rocked every 5 min. VSV-ΔM51-GFP in MEM without FBS at a cell-line specific MOI of 0.001 was added and the plate was incubated for 1 h with rocking every 10 min. The mixture was aspirated and wells washed 3 times with PBS. For ruxolitinib-treated wells, MEM with 5% FBS, 0.1% DMSO and 2.5 μM ruxolitinib was added. For wells without ruxolitinib treatment, MEM with 5% FBS and 0.1% DMSO was added. The plate was incubated at 37°C. GFP fluorescence was measured at regular intervals (CytoFluor Series 4000, excitation filter of 485/20 nm, emission 530/25 nm, gain=63; Applied Biosystems). Cell viability assay (MTT) was performed 3 days p.i. To examine the effects of polycations on VSV infectivity by FACS analysis, HPAF-II cells were seeded in a 6-well plate such that they were approximately 80% confluent at the time of treatment. Cells were washed once with PBS. For each test condition, DEAE-dextran or polybrene in MEM without FBS at a concentration of 10 μg/mL was dispensed appropriately. For control and ruxolitinib wells, MEM without FBS was added. The plate was incubated at 37 °C for 30 min during which it was rocked every 5 min. VSV-ΔM51-GFP in MEM without FBS at MOI 0.001 was added and incubated for 1 h with rocking every 10 min. The mixture was aspirated and wells were washed 3 times with PBS. For ruxolitinib-treated wells, MEM with 5% FBS, 0.1% DMSO and 2.5 μM ruxolitinib was added. For wells without ruxolitinib treatment, MEM with 5% FBS and 0.1% DMSO was added. Wells were incubated at 37 °C. At 18 h p.i., cells were washed once with PBS, then trypsinized and resuspended in MEM with 10% FBS. The mixture was

33

792   transferred to flow cytometry tubes and spun at 2000 rpm for 2 min. The supernatant was

793   aspirated and pellet was washed with PBS, then spun again at 2000 rpm for 2 min. The

794   pellet was fixed with 500 μL of 4% paraformaldehyde and kept on ice for 15 min. After

795   another round of centrifugation, the pellet was re-suspended in PBS and kept on ice. Cells

796   were analyzed on a LSR Fortessa cell analyser (BD Bioscience), and the data were

797   analyzed with FlowJo software (Treestar).

798

799   **Statistical analysis.** All statistical analyses were performed using GraphPad Prism 7.0a

800   software. Tests used are indicated in the legends of the figures.

801

802   **ACKNOWLEDGEMENTS**

813

814   **REFERENCES**

815 1. **Orloff M.** 2016. Spotlight on talimogene laherparepvec for the treatment of
816   melanoma lesions in the skin and lymph nodes. Oncolytic Virother **5:**91-98.

817 2. **Rehman H, Silk AW, Kane MP, Kaufman HL.** 2016. Into the clinic: Talimogene
818   laherparepvec (T-VEC), a first-in-class intratumoral oncolytic viral therapy. J
819   Immunother Cancer **4:**53.

820 3. **Donina S, Strele I, Proboka G, Auzins J, Alberts P, Jonsson B, Venskus D,
821   Muceniece A.** 2015. Adapted ECHO-7 virus Rigvir immunotherapy (oncolytic
822   virotherapy) prolongs survival in melanoma patients after surgical excision of the
823   tumour in a retrospective study. Melanoma Res **25:**421-426.

824 4. **Garber K.** 2006. China approves world's first oncolytic virus therapy for cancer
825   treatment. J Natl Cancer Inst **98:**298-300.

826 5. **Hastie E, Grdzelishvili VZ.** 2012. Vesicular stomatitis virus as a flexible platform for
827   oncolytic virotherapy against cancer. J Gen Virol **93:**2529-2545.

828 6. **Simovic B, Walsh SR, Wan Y.** 2015. Mechanistic insights into the oncolytic activity
829   of vesicular stomatitis virus in cancer immunotherapy. Oncolytic Virother **4:**157-167.

830 7. **Hastie E, Cataldi M, Marriott I, Grdzelishvili VZ.** 2013. Understanding and altering
831   cell tropism of vesicular stomatitis virus. Virus Res **176:**16-32.

832 8. **Stojdl DF, Lichty BD, Knowles S, Marius R, Atkins H, Sonenberg N, Bell JC.**
833   2000. Exploiting tumor-specific defects in the interferon pathway with a previously
834   unknown oncolytic virus. Nat Med **6:**821-825.

835 9. **Stojdl DF, Lichty BD, tenOever BR, Paterson JM, Power AT, Knowles S, Marius
836   R, Reynard J, Poliquin L, Atkins H, Brown EG, Durbin RK, Durbin JE, Hiscott J,
837   Bell JC.** 2003. VSV strains with defects in their ability to shutdown innate immunity
838   are potent systemic anti-cancer agents. Cancer Cell **4:**263-275.

839 10. **Lichty BD, Power AT, Stojdl DF, Bell JC.** 2004. Vesicular stomatitis virus: re-
840   inventing the bullet. Trends Mol Med **10:**210-216.

841 11. **Barber GN.** 2004. Vesicular stomatitis virus as an oncolytic vector. Viral Immunol
842   **17:**516-527.

843 12. **Wang BX, Rahbar R, Fish EN.** 2011. Interferon: current status and future prospects
844   in cancer therapy. J Interferon Cytokine Res **31:**545-552.

845 13. **Petersen JM, Her LS, Varvel V, Lund E, Dahlberg JE.** 2000. The matrix protein of
846   vesicular stomatitis virus inhibits nucleocytoplasmic transport when it is in the nucleus
847   and associated with nuclear pore complexes. Mol Cel Biol **20:**8590-8601.

848   14.   **Clarke DK NF, Lee M, Johnson JE, Wright K, Calderon P, Guo M, Natuk R,**
849   **Cooper D, Hendry RM, Udem SA.** 2007. Synergistic attenuation of vesicular
850   stomatitis virus by combination of specific G gene truncations and N gene
851   translocations. J Virol **81:**2056-2064.

852   15.   **Johnson JE, Nasar F, Coleman JW, Price RE, Javadian A, Draper K, Lee M,**
853   **Reilly PA, Clarke DK, Hendry RM, Udem SA.** 2007. Neurovirulence properties of
854   recombinant vesicular stomatitis virus vectors in non-human primates. Virology
855   **360:**36-49.

856   16.   **Finkelshtein D, Werman A, Novick D, Barak S, Rubinstein M.** 2013. LDL receptor
857   and its family members serve as the cellular receptors for vesicular stomatitis virus.
858   Proc Natl Acad Sci USA **110:**7306-7311.

859   17.   **Schlegel R, Tralka TS, Willingham MC, Pastan I.** 1983. Inhibition of VSV binding
860   and infectivity by phosphatidylserine: is phosphatidylserine a VSV-binding site? Cell
861   **32:**639-646.

862   18.   **Coil DA, Miller AD.** 2004. Phosphatidylserine is not the cell surface receptor for
863   vesicular stomatitis virus. J Virol **78:**10920-10926.

864   19.   **Carneiro FA, Lapido-Loureiro PA, Cordo SM, Stauffer F, Weissmuller G,**
865   **Bianconi ML, Juliano MA, Juliano L, Bisch PM, Da Poian AT.** 2006. Probing the
866   interaction between vesicular stomatitis virus and phosphatidylserine. Eur Biophys J
867   **35:**145-154.

868   20.   **Schloemer RH, Wagner RR.** 1975. Cellular adsorption function of the
869   sialoglycoprotein of vesicular stomatitis virus and its neuraminic acid. J Virol **15:**882-
870   893.

871   21.   **Guibinga GH, Miyanohara A, Esko JD, Friedmann T.** 2002. Cell surface heparan
872   sulfate is a receptor for attachment of envelope protein-free retrovirus-like particles
873   and VSV-G pseudotyped MLV-derived retrovirus vectors to target cells. Mol Ther
874   **5:**538-546.

875   22.   **Pearson AS, Koch PE, Atkinson N, Xiong M, Finberg RW, Roth JA, Fang B.**
876   1999. Factors limiting adenovirus-mediated gene transfer into human lung and
877   pancreatic cancer cell lines. Clinical Cancer Res **5:**4208-4213.

878   23.   **Stathis A, Moore MJ.** 2010. Advanced pancreatic carcinoma: current treatment and
879   future challenges. Nat Rev Clin Oncol **7:**163-172.

880   24.   **Rahib L, Smith BD, Aizenberg R, Rosenzweig AB, Fleshman JM, Matrisian LM.**
881   2014. Projecting cancer incidence and deaths to 2030: the unexpected burden of
882   thyroid, liver, and pancreas cancers in the United States. Cancer Res **74:**2913-2921.
883   25.   **Wennier S, Li S, McFadden G.** 2011. Oncolytic virotherapy for pancreatic cancer.
884   Expert Rev Mol Med **13:**e18.
885   26.   **Murphy AM, Besmer DM, Moerdyk-Schauwecker M, Moestl N, Ornelles DA,**
886   **Mukherjee P, Grdzelishvili VZ.** 2012. Vesicular stomatitis virus as an oncolytic
887   agent against pancreatic ductal adenocarcinoma. J Virol **86:**3073-3087.
888   27.   **Moerdyk-Schauwecker M, Shah NR, Murphy AM, Hastie E, Mukherjee P,**
889   **Grdzelishvili VZ.** 2013. Resistance of pancreatic cancer cells to oncolytic vesicular
890   stomatitis virus: role of type I interferon signaling. Virology **436:**221-234.
891   28.   **Cataldi M, Shah NR, Felt SA, Grdzelishvili VZ.** 2015. Breaking resistance of
892   pancreatic cancer cells to an attenuated vesicular stomatitis virus through a novel
893   activity of IKK inhibitor TPCA-1. Virology **485:**340-354.
894   29.   **Hastie E, Cataldi M, Moerdyk-Schauwecker MJ, Felt SA, Steuerwald N,**
895   **Grdzelishvili VZ.** 2016. Novel biomarkers of resistance of pancreatic cancer cells to
896   oncolytic vesicular stomatitis virus. Oncotarget **7:**61601-61618.
897   30.   **Felt SA, Moerdyk-Schauwecker MJ, Grdzelishvili VZ.** 2015. Induction of apoptosis
898   in pancreatic cancer cells by vesicular stomatitis virus. Virology **474:**163-173.
899   31.   **Wollmann G, Rogulin V, Simon I, Rose JK, van den Pol AN.** 2010. Some
900   attenuated variants of vesicular stomatitis virus show enhanced oncolytic activity
901   against human glioblastoma cells relative to normal brain cells. J Virol **84:**1563-1573.
902   32.   **Ahmed M, McKenzie MO, Puckett S, Hojnacki M, Poliquin L, Lyles DS.** 2003.
903   Ability of the matrix protein of vesicular stomatitis virus to suppress beta interferon
904   gene expression is genetically correlated with the inhibition of host RNA and protein
905   synthesis. J Virol **77:**4646-4657.
906   33.   **Kopecky SA, Willingham MC, Lyles DS.** 2001. Matrix protein and another viral
907   component contribute to induction of apoptosis in cells infected with vesicular
908   stomatitis virus. J Virol **75:**12169-12181.
909   34.   **Hastie E, Cataldi M, Steuerwald N, Grdzelishvili VZ.** 2015. An unexpected
910   inhibition of antiviral signaling by virus-encoded tumor suppressor p53 in pancreatic
911   cancer cells. Virology **483:**126-140.

912 35. **Finkelshtein D, Werman A, Novick D, Barak S, Rubinstein M.** 2013. LDL receptor
913   and its family members serve as the cellular receptors for vesicular stomatitis virus.
914   Proc Natl Acad Sci U S A **110:**7306-7311.

915 36. **Ammayappan A, Peng KW, Russell SJ.** 2013. Characteristics of oncolytic vesicular
916   stomatitis virus displaying tumor-targeting ligands. J Virol **87:**13543-13555.

917 37. **Amirache F, Levy C, Costa C, Mangeot PE, Torbett BE, Wang CX, Negre D,**
918   **Cosset FL, Verhoeyen E.** 2014. Mystery solved: VSV-G-LVs do not allow efficient
919   gene transfer into unstimulated T cells, B cells, and HSCs because they lack the LDL
920   receptor. Blood **123:**1422-1424.

921 38. **Guillaumond F, Bidaut G, Ouaissi M, Servais S, Gouirand V, Olivares O, Lac S,**
922   **Borge L, Roques J, Gayet O, Pinault M, Guimaraes C, Nigri J, Loncle C, Lavaut**
923   **MN, Garcia S, Tailleux A, Staels B, Calvo E, Tomasini R, Iovanna JL, Vasseur S.**
924   2015. Cholesterol uptake disruption, in association with chemotherapy, is a promising
925   combined metabolic therapy for pancreatic adenocarcinoma. Proc Natl Acad Sci U S
926   A **112:**2473-2478.

927 39. **Tolleshaug H, Goldstein JL, Schneider WJ, Brown MS.** 1982. Posttranslational
928   processing of the LDL receptor and its genetic disruption in familial
929   hypercholesterolemia. Cell **30:**715-724.

930 40. **Tolleshaug H, Hobgood KK, Brown MS, Goldstein JL.** 1983. The LDL receptor
931   locus in familial hypercholesterolemia: multiple mutations disrupt transport and
932   processing of a membrane receptor. Cell **32:**941-951.

933 41. **Maxwell KN, Fisher EA, Breslow JL.** 2005. Overexpression of PCSK9 accelerates
934   the degradation of the LDLR in a post-endoplasmic reticulum compartment. Proc Natl
935   Acad Sci U S A **102:**2069-2074.

936 42. **Marais AD.** 2004. Familial hypercholesterolaemia. Clin Biochem Rev **25:**49-68.

937 43. **Tveten K, Ranheim T, Berge KE, Leren TP, Kulseth MA.** 2006. Analysis of
938   alternatively spliced isoforms of human LDL receptor mRNA. Clin Chim Acta
939   **373:**151-157.

940 44. **Pahan K.** 2006. Lipid-lowering drugs. Cell Mol Life Sci **63:**1165-1178.

941 45. **Vaziri ND, Liang K.** 2004. Effects of HMG-CoA reductase inhibition on hepatic
942   expression of key cholesterol-regulatory enzymes and receptors in nephrotic
943   syndrome. Am J Nephrol **24:**606-613.

944   46.   **Santos RD, Watts GF.** 2015. Familial hypercholesterolaemia: PCSK9 inhibitors are
945   coming. Lancet **385:**307-310.

946   47.   **McNutt MC, Kwon HJ, Chen C, Chen JR, Horton JD, Lagace TA.** 2009.
947   Antagonism of secreted PCSK9 increases low density lipoprotein receptor expression
948   in HepG2 cells. J Biol Chem **284:**10561-10570.

949   48.   **Wu M, Dong B, Cao A, Li H, Liu J.** 2012. Delineation of molecular pathways that
950   regulate hepatic PCSK9 and LDL receptor expression during fasting in
951   normolipidemic hamsters. Atherosclerosis **224:**401-410.

952   49.   **Chen Y, Ruan XZ, Li Q, Huang A, Moorhead JF, Powis SH, Varghese Z.** 2007.
953   Inflammatory cytokines disrupt LDL-receptor feedback regulation and cause statin
954   resistance: a comparative study in human hepatic cells and mesangial cells. Am J
955   Physiol Renal Physiol **293:**F680-687.

956   50.   **Ye Q, Lei H, Fan Z, Zheng W, Zheng S.** 2014. Difference in LDL receptor feedback
957   regulation in macrophages and vascular smooth muscle cells: foam cell
958   transformation under inflammatory stress. Inflammation **37:**555-565.

959   51.   **Russell DW, Yamamoto T, Schneider WJ, Slaughter CJ, Brown MS, Goldstein
960   JL.** 1983. cDNA cloning of the bovine low density lipoprotein receptor: feedback
961   regulation of a receptor mRNA. Proc Natl Acad Sci U S A **80:**7501-7505.

962   52.   **Fischer DG, Novick D, Cohen B, Rubinstein M.** 1994. Isolation and
963   characterization of a soluble form of the LDL receptor, an interferon-induced antiviral
964   protein. Proc Soc Exp Biol Med **206:**228-232.

965   53.   **Fischer DG, Tal N, Novick D, Barak S, Rubinstein M.** 1993. An antiviral soluble
966   form of the LDL receptor induced by interferon. Science **262:**250-253.

967   54.   **Kniss DA, Summerfield TL.** 2014. Discovery of HeLa Cell Contamination in HES
968   Cells: Call for Cell Line Authentication in Reproductive Biology Research. Reprod Sci
969   **21:**1015-1019.

970   55.   **Kingsley DM, Kozarsky KF, Hobbie L, Krieger M.** 1986. Reversible defects in O-
971   linked glycosylation and LDL receptor expression in a UDP-Gal/UDP-GalNAc 4-
972   epimerase deficient mutant. Cell **44:**749-759.

973   56.   **Kozarsky K, Kingsley D, Krieger M.** 1988. Use of a mutant cell line to study the
974   kinetics and function of O-linked glycosylation of low density lipoprotein receptors.
975   Proc Natl Acad Sci U S A **85:**4335-4339.

976 57. **Conti C, Mastromarino P, Riccioli A, Orsi N.** 1991. Electrostatic interactions in the
977   early events of VSV infection. Res Virol **142:**17-24.

978 58. **Bailey CA, Miller DK, Lenard J.** 1984. Effects of DEAE-dextran on infection and
979   hemolysis by VSV. Evidence that nonspecific electrostatic interactions mediate
980   effective binding of VSV to cells. Virology **133:**111-118.

981 59. **Matlin KS, Reggio H, Helenius A, Simons K.** 1982. Pathway of vesicular stomatitis
982   virus entry leading to infection. J Mol Biol **156:**609-631.

983 60. **Reiser J, Harmison G, Kluepfel-Stahl S, Brady RO, Karlsson S, Schubert M.**
984   1996. Transduction of nondividing cells using pseudotyped defective high-titer HIV
985   type 1 particles. Proc Natl Acad Sci U S A **93:**15266-15271.

986 61. **Yee JK, Friedmann T, Burns JC.** 1994. Generation of high-titer pseudotyped
987   retroviral vectors with very broad host range. Methods Cell Biol **43 Pt A:**99-112.

988 62. **Denning W, Das S, Guo S, Xu J, Kappes JC, Hel Z.** 2013. Optimization of the
989   transductional efficiency of lentiviral vectors: effect of sera and polycations. Mol
990   Biotechnol **53:**308-314.

991 63. **Davis CG, Elhammer A, Russell DW, Schneider WJ, Kornfeld S, Brown MS,**
992   **Goldstein JL.** 1986. Deletion of clustered O-linked carbohydrates does not impair
993   function of low density lipoprotein receptor in transfected fibroblasts. J Biol Chem
994   **261:**2828-2838.

995 64. **Yoshimura A, Yoshida T, Seguchi T, Waki M, Ono M, Kuwano M.** 1987. Low
996   binding capacity and altered O-linked glycosylation of low density lipoprotein receptor
997   in a monensin-resistant mutant of Chinese hamster ovary cells. J Biol Chem
998   **262:**13299-13308.

999 65. **Kalra AV, Campbell RB.** 2009. Mucin overexpression limits the effectiveness of 5-
1000   FU by reducing intracellular drug uptake and antineoplastic drug effects in pancreatic
1001   tumours. Eur J Cancer **45:**164-173.

1002 66. **Kalra AV, Campbell RB.** 2007. Mucin impedes cytotoxic effect of 5-FU against
1003   growth of human pancreatic cancer cells: overcoming cellular barriers for therapeutic
1004   gain. Br J Cancer **97:**910-918.

1005 67. **Davis HE, Morgan JR, Yarmush ML.** 2002. Polybrene increases retrovirus gene
1006   transfer efficiency by enhancing receptor-independent virus adsorption on target cell
1007   membranes. Biophys Chem **97:**159-172.

1008   68. **Tiera MJ, Shi Q, Winnik FM, Fernandes JC.** 2011. Polycation-based gene therapy:
1009   current knowledge and new perspectives. Curr Gene Ther **11:**288-306.

1010   69. **Aied A, Greiser U, Pandit A, Wang W.** 2013. Polymer gene delivery: overcoming
1011   the obstacles. Drug Discov Today **18:**1090-1098.

1012   70. **Kaplan JM, Pennington SE, St George JA, Woodworth LA, Fasbender A,**
1013   **Marshall J, Cheng SH, Wadsworth SC, Gregory RJ, Smith AE.** 1998. Potentiation
1014   of gene transfer to the mouse lung by complexes of adenovirus vector and
1015   polycations improves therapeutic potential. Hum Gene Ther **9:**1469-1479.

1016   71. **McKay TR, MacVinish LJ, Carpenter B, Themis M, Jezzard S, Goldin R, Pavirani**
1017   **A, Hickman ME, Cuthbert AW, Coutelle C.** 2000. Selective in vivo transfection of
1018   murine biliary epithelia using polycation-enhanced adenovirus. Gene Ther **7:**644-652.

1019   72. **Gregory LG, Harbottle RP, Lawrence L, Knapton HJ, Themis M, Coutelle C.**
1020   2003. Enhancement of adenovirus-mediated gene transfer to the airways by DEAE
1021   dextran and sodium caprate in vivo. Mol Ther **7:**19-26.

1022   73. **Kushwah R, Oliver JR, Cao H, Hu J.** 2007. Nacystelyn enhances adenoviral vector-
1023   mediated gene delivery to mouse airways. Gene Ther **14:**1243-1248.

1024   74. **Monnery BD, Wright M, Cavill R, Hoogenboom R, Shaunak S, Steinke JH,**
1025   **Thanou M.** 2017. Cytotoxicity of polycations: Relationship of molecular weight and
1026   the hydrolytic theory of the mechanism of toxicity. Int J Pharm **521:**249-258.

1027   75. **Zarogoulidis P, Hohenforst-Schmidt W, Darwiche K, Krauss L, Sparopoulou D,**
1028   **Sakkas L, Gschwendtner A, Huang H, Turner FJ, Freitag L, Zarogoulidis K.**
1029   2013. 2-diethylaminoethyl-dextran methyl methacrylate copolymer nonviral vector:
1030   still a long way toward the safety of aerosol gene therapy. Gene Ther **20:**1022-1028.

1031   76. **Simmons CF, Jr., Rennke HG, Humes HD.** 1981. Acute renal failure induced by
1032   diethylaminoethyl dextran: importance of cationic charge. Kidney Int **19:**424-430.

1033   77. **Seitz B, Baktanian E, Gordon EM, Anderson WF, LaBree L, McDonnell PJ.** 1998.
1034   Retroviral vector-mediated gene transfer into keratocytes: in vitro effects of polybrene
1035   and protamine sulfate. Graefes Arch Clin Exp Ophthalmol **236:**602-612.

1036   78. **Lin P, Correa D, Lin Y, Caplan AI.** 2011. Polybrene inhibits human mesenchymal
1037   stem cell proliferation during lentiviral transduction. PLoS One **6:**e23891.

1038   79. **Park TG, Jeong JH, Kim SW.** 2006. Current status of polymeric gene delivery
1039   systems. Adv Drug Deliv Rev **58:**467-486.

1040 80. **Vaddi K, Sarlis NJ, Gupta V.** 2012. Ruxolitinib, an oral JAK1 and JAK2 inhibitor, in
1041   myelofibrosis. Expert Opin Pharmacother **13:**2397-2407.

1042 81. **Dold C, Rodriguez Urbiola C, Wollmann G, Egerer L, Muik A, Bellmann L, Fiegl**
1043   **H, Marth C, Kimpel J, von Laer D.** 2016. Application of interferon modulators to
1044   overcome partial resistance of human ovarian cancers to VSV-GP oncolytic viral
1045   therapy. Mol Ther Oncolytics **3:**16021.

1046 82. **Nguyên TL AH, Arguello M, Breitbach C, Leveille S, Diallo JS, Yasmeen A,**
1047   **Bismar TA, Kirn D, Falls T, Snoulten VE, Vanderhyden BC, Werier J, Atkins H,**
1048   **Vähä-Koskela MJ, Stojdl DF, Bell JC, Hiscott J.** 2008. Chemical targeting of the
1049   innate antiviral response by histone deacetylase inhibitors renders refractory cancers
1050   sensitive to viral oncolysis. Proc Natl Acad Sci U S A **105:**14981-14986.

1051 83. **Shulak L, Beljanski V, Chiang C, Dutta SM, Van Grevenynghe J, Belgnaoui SM,**
1052   **Nguyen TL, Di Lenardo T, Semmes OJ, Lin R, Hiscott J.** 2014. Histone
1053   deacetylase inhibitors potentiate vesicular stomatitis virus oncolysis in prostate
1054   cancer cells by modulating NF-kappaB-dependent autophagy. J Virol **88:**2927-2940.

1055 84. **Shestakova E, Bandu MT, Doly J, Bonnefoy E.** 2001. Inhibition of histone
1056   deacetylation induces constitutive derepression of the beta interferon promoter and
1057   confers antiviral activity. J Virol **75:**3444-3452.

1058 85. **Hastie E, Besmer DM, Shah NR, Murphy AM, Moerdyk-Schauwecker M,**
1059   **Molestina C, Roy LD, Curry JM, Mukherjee P, Grdzelishvili VZ.** 2013. Oncolytic
1060   Vesicular Stomatitis Virus in an Immunocompetent Model of MUC1-Positive or
1061   MUC1-Null Pancreatic Ductal Adenocarcinoma. J Virol **87:**10283-10294.

1062 86. **Moerdyk-Schauwecker M, Hwang SI, Grdzelishvili VZ.** 2014. Cellular proteins
1063   associated with the interior and exterior of vesicular stomatitis virus virions. PLoS
1064   One **9:**e104688.

1065 87. **Iwamura T, Katsuki T, Ide K.** 1987. Establishment and characterization of a human
1066   pancreatic cancer cell line (SUIT-2) producing carcinoembryonic antigen and
1067   carbohydrate antigen 19-9. Jpn J Cancer Res **78:**54-62.

1068 88. **Nguyen AT, Hirama T, Chauhan V, Mackenzie R, Milne R.** 2006. Binding
1069   characteristics of a panel of monoclonal antibodies against the ligand binding domain
1070   of the human LDLr. J Lipid Res **47:**1399-1405.

1071   89.   **Beisiegel U, Schneider WJ, Brown MS, Goldstein JL.** 1982. Immunoblot analysis

1072   of low density lipoprotein receptors in fibroblasts from subjects with familial

1073   hypercholesterolemia. J Biol Chem **257:**13150-13156.

1074   90.   **van Driel IR, Goldstein JL, Sudhof TC, Brown MS.** 1987. First cysteine-rich repeat

1075   in ligand-binding domain of low density lipoprotein receptor binds Ca2+ and

1076   monoclonal antibodies, but not lipoproteins. J Biol Chem **262:**17443-17449.

1077
1078
1079

1080

1081

1082

1083

1084

1085

1086

1087

1088   **FIGURE LEGENDS**

1089   **Figure1: VSV attachment to PDAC cell lines.** (A) For VSV attachment to cells in

1090   suspension, cells were detached with PBS with 0.2% EDTA and incubated for 1h at 4°C

1091   with VSV-ΔM51-eqFP650. After incubation with VSV-G primary antibody and APC-

1092   conjugated secondary antibody, cells were analyzed by FACS using the APC-A channel.

1093   "Control" cells were mock-treated (without VSV), and primary and secondary antibodies

1094   were used. "VSV attachment" cells were incubated with various amounts of VSV (the

1095   indicated MOIs are based on virus titration on MIA PaCa-2). Gated populations are positive

1096   for VSV attachment (% of VSV-positive cells is indicated above the gate line). MFI stands

1097   for "Mean Fluorescent Intensity" of each population and was calculated by FlowJo software

1098   (Treestar). (B) For VSV attachment to cells in monolayer, cell monolayers were incubated

1099   for 1h at 4°C ("Attachment") or for additional 8h at 37°C ("Replication") with VSV-ΔM51-

1100   eqFP650. Protein was isolated and analyzed by western blotting. MOI is indicated on top

1101   and is based on MIA PaCa-2. Protein (kDa) product sizes are indicated on the right.

1102   Coomassie blue stain was used to indicate equal loading. (C) Cells in monolayer were

1103   incubated for 15 min, 30 min or 1h at 4°C with VSV-ΔM51-eqFP650 or mock-treated

1104   ("Mock"). MOI used is 50 based on MIA PaCa-2. Protein (kDa) product sizes are indicated

1105   on the right. GAPDH and Coomassie blue stain were used to confirm equal loading.

1106

1107   **Figure 2: LDLR expression and functionality in PDAC cell lines.** (A) Total protein

1108   lysates were isolated from untreated cells and analyzed by ELISA for LDLR levels. LDLR

1109   levels were normalized to total protein levels. Assay was done in triplicate and data

1110   represent the mean ± standard error of mean. Cell lines were compared using a 1-way

1111   ANOVA followed by the Dunnett posttest for comparison to HPAF-II. **, $P<0.01$; ****,

1112 $p<0.0001$. (B) Cell monolayers were incubated for 1h at 4°C with various amounts of VSV-

1113   ΔM51-eqFP650 (the indicated MOIs are based on virus titration on MIA PaCa-2). Protein

1114   lysates were analyzed for LDLR and VSV proteins by western blot. Protein (kDa) product

1115   sizes are indicated on the right. GAPDH and Coomassie blue stain were used to confirm

1116   equal loading. (C) For LDLR cell surface expression, cells were kept on ice and not

1117   permeabilized and not fixed. After incubation with anti-LDLR primary antibody and APC-

1118   conjugated secondary antibody cells were analyzed by FACS using the APC-A channel.

1119   "Control" cells were incubated with secondary antibody only. "LDLR" cells were incubated

1120   with primary and secondary antibody. Gated populations are positive for LDLR (% of LDLR-

1121   positive cells is indicated above the gate line). MFI stands for "Mean Fluorescent Intensity"

1122   of each population and was calculated by FlowJo software (Treestar). Data are

44

1123   representative of 3 independent experiments. (D) For the LDL uptake assay, cells were

1124   incubated for 4 h with fluorescently labeled LDL and then analyzed by FACS using the PE-A

1125   channel. "Control": fluorescently labeled LDL was not added; "LDL": fluorescently labeled

1126   LDL was added. Gated populations are positive for LDL uptake (% of LDL-positive cells is

1127   indicated above the gate line). MFI stands for "Mean Fluorescent Intensity" for each

1128   population and was calculated by FlowJo software (Treestar). Data are representative of 3

1129   independent experiments.

1130

1131   **Figure 3: Effect of statins on LDLR expression, LDL uptake and VSV attachment.** (A)

1132   Cells were pretreated with statins (10 µM) or SBC-115076 (10 µM) or LDLR (25 µg/ml) or

1133   ruxolitinib (2.5 µM) for 24 h and were then incubated for 1h at 4°C with VSV-ΔM51-

1134   eqFP650. MOI was 250 based on MIA PaCa-2. Protein isolates were used for western blot

1135   analyzes. Protein (kDa) product sizes are indicated on the right. GAPDH and Coomassie

1136   blue stain were used to indicate equal loading. (B) Cells were pretreated with statins or

1137   other conditions at the same concentration as above for 24h and then incubated for 4 h at

1138   37°C with fluorescently labeled LDL. Samples were analyzed by FACS using the PE-A

1139   channel. "Control": fluorescently labeled LDL was not added; "LDL": fluorescently labeled

1140   LDL was added. Treatments are indicated on top of each histogram. Gated populations are

1141   positive for LDL uptake (% of LDL-positive cells is indicated above the gate line). MFI stands

1142   for "Mean Fluorescent Intensity" for each population and was calculated by FlowJo software

1143   (Treestar). (C) Cells were pretreated with statins at the same concentration as above for

1144   24h and then analyzed for LDLR cell surface expression. Cells were kept on ice and not

1145   permeabilized and not fixed. After incubation with anti-LDLR primary antibody and APC-

1146   conjugated secondary antibody cells were analyzed by FACS using the APC-A channel.

1147   "Control" cells were incubated with secondary antibody only. "LDLR" cells were incubated

45

1148   with primary and secondary antibody. Gated populations are positive for LDLR (% of LDLR-

1149   positive cells is indicated above the gate line). MFI stands for "Mean Fluorescent Intensity"

1150   of each population and was calculated by FlowJo software (Treestar). (D) Cells were

1151   pretreated with statins at the same concentration as above for 24h and then analyzed for

1152   LDLR cell surface expression. Cells were kept on ice and not permeabilized and not fixed.

1153   After incubation with anti-LDLR primary antibody and AlexaFluor488-conjugated secondary

1154   antibody cells were observed by microscopy and picture were taken.

1155

1156   **Figure 4: Effect of type I interferon and sLDLR on VSV attachment.** (A) Cells were

1157   pretreated with ruxolitinib (2.5 μM) for 24h and then incubated for 1h at 4°C with VSV-

1158   ΔM51-eqFP650 (MOI 20 based on MIA PaCa-2). Protein was isolated and analyzed by

1159   western blot. Protein (kDa) product sizes are indicated on the right. GAPDH was used to

1160   indicate equal loading. (B) VSV-ΔM51-eqFP650 alone or VSV-ΔM51-eqFP650 with soluble

1161   LDLR (1 μg/ml) was added on PDAC cell line and plaques were counted the next day to

1162   determine effect on infectivity. Data are representative of 3 independent experiments and

1163   shows the mean ± standard error of mean. Conditions were compared using an unpaired t-

1164   test. ****, $p<0.0001$. (C) Cells were grown in culture for 24 h and then media were used to

1165   determine sLDLR levels by ELISA. Soluble LDLR levels were normalized by total protein.

1166   Assay was done in triplicate and data represent the mean ± standard error of mean.

1167   Conditions were compared using a 1-way ANOVA followed by the Dunnett posttest for

1168   comparison to HPAF-II. **, $P<0.01$; ***, $p<0.001$. (D-E) Cells were treated with IFN (5000

1169   U/ml), ruxolitinib (2.5 μM) or IFN (5000 U/ml)/ruxolitinib (2.5 μM) for 24 h. Medium or protein

1170   isolates were then used to determine effect on sLDLR or LDLR levels by ELISA. LDLR and

1171   sLDLR levels were normalized by total protein. Assay was done in triplicate and data

1172   represent the mean ± standard error of mean. Conditions were compared using a 1-way

46

1173 ANOVA followed by the Dunnett posttest for comparison to the control. *, p<0.05; ***,

1174 p<0.001; ****, p<0.0001. (F) Cells were pretreated with ruxolitininb (2.5 µM) for 24h and

1175 then incubated for 4 h at 37°C with fluorescently labeled LDL. Samples were analyzed by

1176 FACS using the PE-A channel. "Control": fluorescently labeled LDL was not added; "LDL":

1177 fluorescently labeled LDL was added. Treatments are indicated on top of each histogram.

1178 The "Mock" sample is the same as in Fig. 3B. Gated populations are positive for LDL uptake

1179 (% of LDL-positive cells is indicated above the gate line). MFI stands for "Mean Fluorescent

1180 Intensity" for each population and was calculated by FlowJo software (Treestar).

1181

1182 **Figure 5: Effect of LDLR digestion by trypsin on VSV attachment.** Cells were treated

1183 with PBS with 0.2% or 0.05% trypsin and then were used for VSV-ΔM51-eqFP650

1184 attachment analysis or protein was isolated to confirm LDLR digestion. (A) For the

1185 attachment assay, after a 1 h incubation at 4°C with VSV-ΔM51-eqFP650 (MOI 125 based

1186 on MIA PaC-2), cells were incubated with anti-VSV-G antibody and APC-conjugated

1187 secondary antibody and analyzed by FACS using the APC-A channel. "Control" cells were

1188 mock-treated (without VSV-ΔM51-eqFP650), and primary and secondary antibodies were

1189 used. "VSV attachment" cells were incubated with VSV-ΔM51-eqFP650. Gated populations

1190 are positive for VSV attachment (% of VSV-positive cells is indicated above the gate line).

1191 MFI stands for "Mean Fluorescent Intensity" of each population and was calculated by

1192 FlowJo software (Treestar). (B) Protein was isolated and analyzed by western blot. Protein

1193 (kDa) product sizes are indicated on the right. GAPDH and Coomassie blue stain were used

1194 to indicate equal loading.

1195

1196 **Figure 6: Effect of polycation treatment on VSV attachment, replication and**

1197 **oncolysis.** (A) Cells were treated with polybrene, DEAE dextran or different pH at the

1198 indicated concentrations and then incubated for 1 h at 37°C with VSV-ΔM51-GFP at the

1199 indicated MOI (based on HPAF-II). (A) GFP fluorescence was analyzed at 46 h p.i. Assay

1200 was done in triplicate and data represent the mean ± standard error of mean. Conditions

1201 were compared using a 1-way ANOVA followed by the Dunnett posttest for comparison to

1202 "+VSV Control". *, $p<0.05$; **, $P<0.01$; ***, $p<0.001$; ****, $p<0.0001$. (B) 5 days p.i. cells were

1203 analyzed for viability by MTT. Assay was done in triplicate and data represent the mean ±

1204 standard error of mean. Conditions were compared using a 1-way ANOVA followed by the

1205 Dunnett posttest for comparison to "+VSV Control". *, $p<0.05$; **, $P<0.01$; ***, $p<0.001$; ****,

1206 $p<0.0001$. (C) Cells were pretreated with polybrene (10 μg/ml) and DEAE-dextran (10

1207 μg/ml) and were then incubated for 1h at 4°C with VSV-ΔM51-eqFP650. MOI was 250

1208 based on MIA PaCa-2. Protein isolates were used for western blot analyzes. Protein (kDa)

1209 product sizes are indicated on the right. GAPDH and Coomassie blue stain were used to

1210 indicate equal loading. Samples were run on the same gel and irrelevant lanes were

1211 removed. (D) Cells in suspension were treated as in (C). MOI was 125 based on MIA PaCa-

1212 2. After incubation with VSV-G primary antibody and APC-conjugated secondary antibody,

1213 cells were analyzed by FACS using the APC-A channel. "Control" cells were mock-treated

1214 (without VSV), and primary and secondary antibodies were used. "VSV attachment" cells

1215 were incubated with various amounts of VSV (the indicated MOIs are based on virus

1216 titration on MIA PaCa-2). Gated populations are positive for VSV attachment (% of VSV-

1217 positive cells is indicated above the gate line). MFI stands for "Mean Fluorescent Intensity"

1218 of each population and was calculated by FlowJo software (Treestar). (E) Cells were

1219 pretreated at the same concentration as above and then incubated for 4 h at 37°C with

1220 fluorescently labeled LDL. Samples were analyzed by FACS using the PE-A channel.

1221 "Control": fluorescently labeled LDL was not added; "LDL": fluorescently labeled LDL was

48

1222   added. Treatments are indicated on top of each histogram. The "Mock" samples are the

1223   same than in Fig. 3B. Gated populations are positive for LDL uptake (% of LDL-positive cells

1224   is indicated above the gate line). MFI stands for "Mean Fluorescent Intensity" for each

1225   population and was calculated by FlowJo software (Treestar).

1226

1227   **Figure 7: Effect of combining polycations with ruxolitinib on VSV infection and**

1228   **oncolysis in HPAF-II.**   Cells were pretreated with 10 µg/ml polybrene or DEAE-dextran or

1229   mock-treated for 30 min, then VSV-ΔM51-GFP at MOI 0.001 (based on HPAF-II) was added

1230   in the presence of polycations (or mock treated) for 1 h at 37 °C, followed by media removal

1231   and washes with PBS, and then incubation in the presence of 2.5 µM ruxolitinib or mock

1232   treatment. VSV infection-associated GFP fluorescence was monitored for 71 h (A), pictures

1233   were taken (B) and then an MTT assay was performed to determine cell viability (C). Assay

1234   was done in triplicate and data represent the mean ± standard error of mean. For GFP

1235   fluorescence conditions were compared using a 2-way ANOVA followed by the Dunnett

1236   posttest for comparison to Mock. ****, $p<0.0001$. The MTT conditions were compared using

1237   a 1-way ANOVA followed by the Dunnett posttest for comparison to Mock (or also

1238   VSV+ruxolitinib for the last three conditions). *, $p<0.05$; ***, $p<0.001$; ****, $p<0.0001$. (D)

1239   Percentage of GFP positive cells was determined at 18 h p.i. by FACS using the FITC-A

1240   channel. Gated populations are positive for GFP. "Control" represents cells alone and "GFP"

1241   represents GFP positive cells in which VSV replication occurred. Gated populations are

1242   positive for VSV replication. MFI stands for "Mean Fluorescent Intensity" for each population

1243   and was calculated by FlowJo software (Treestar).

1244

1245   **Figure 8: Effect of combining polycations with ruxolitinib on VSV infection oncolysis**

49

1246 **in other PDAC cell lines.** Cells were pretreated with 10 μg/ml polybrene or DEAE-dextran

1247 or mock-treated for 30 min, then VSV-ΔM51-GFP at MOI 0.001 (cell line specific) was

1248 added in the presence of polycations (or mock treated) for 1 h at 37 °C, followed by media

1249 removal and washes with PBS, and then incubation in the presence of 2.5 μM ruxolitinib or

1250 mock treatment. VSV infection-associated GFP fluorescence was monitored for 68 h and

1251 then an MTT assay was performed to determine cell viability. Assay was done in triplicate

1252 and data represent the mean ± standard error of mean. For GFP fluorescence conditions

1253 were compared using a 2-way ANOVA followed by the Dunnett posttest for comparison to

1254 Mock. ****, $p<0.0001$. The MTT conditions were compared using a 1-way ANOVA followed

1255 by the Dunnett posttest for comparison to Mock (or also to VSV+ruxolitinib for the last three

1256 conditions). *, $p<0.05$; ***, $p<0.001$; ****, $p<0.0001$.
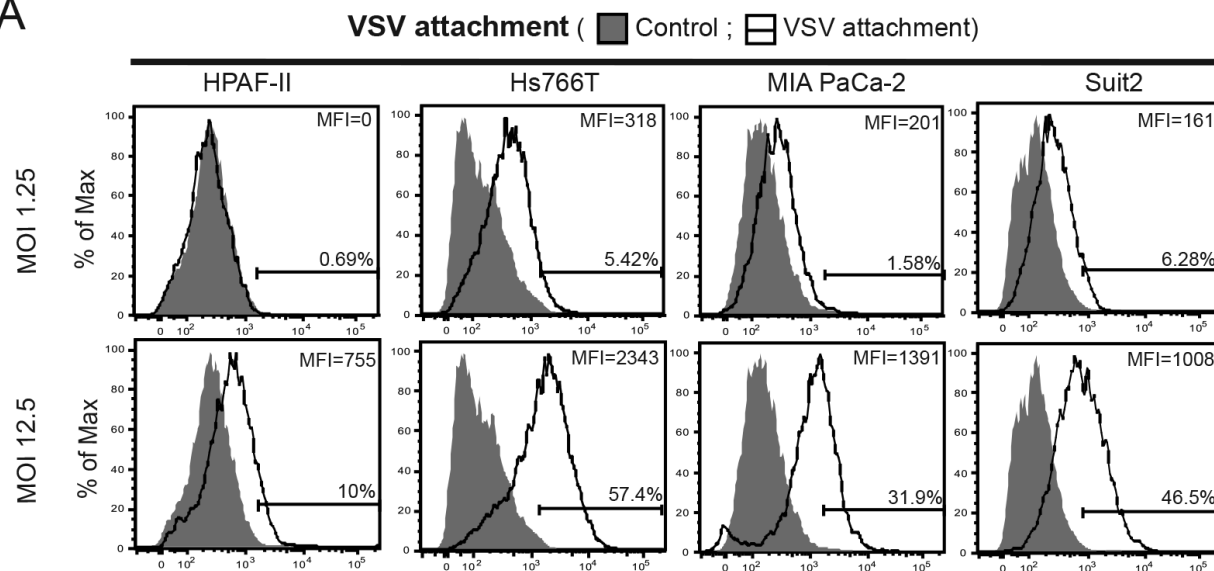
1257

1258 **Figure 9: Proposed schematics of breaking resistance of PDAC cells to VSV by**

1259 **treating cells with polycations and ruxolitinib.** Treatment conditions are indicated

1260 underneath each well (on the left). Green cells represent infected cancer cells. On the right,

1261 the effect of these treatments on VSV characteristics (attachment, replication and
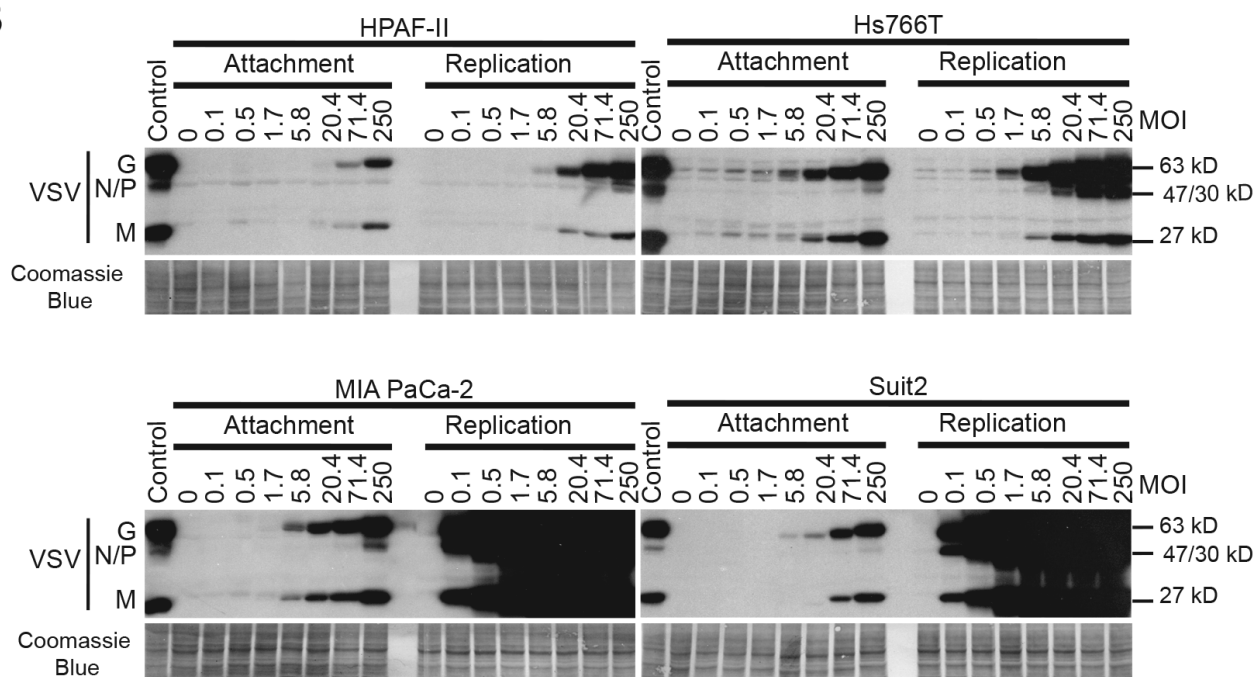
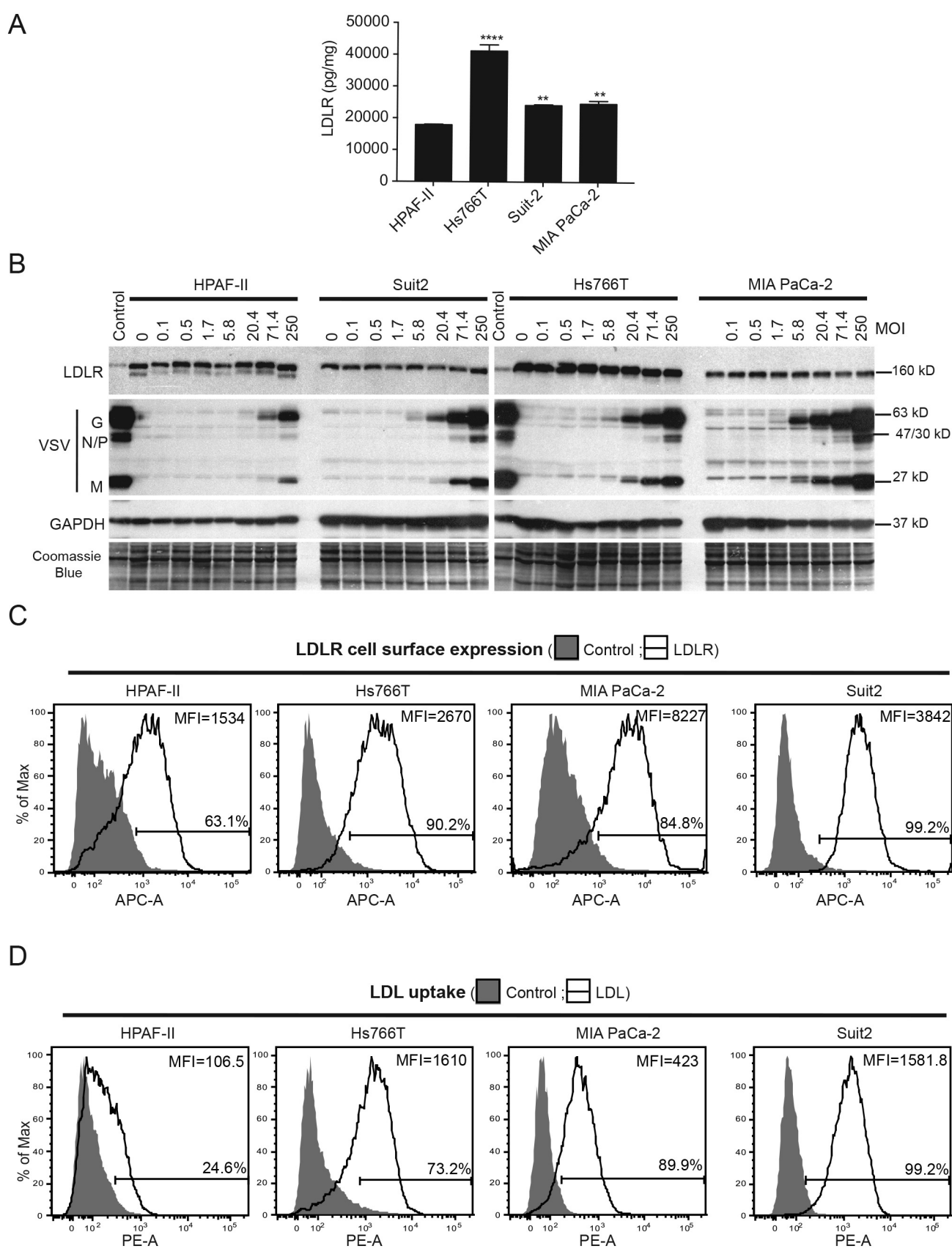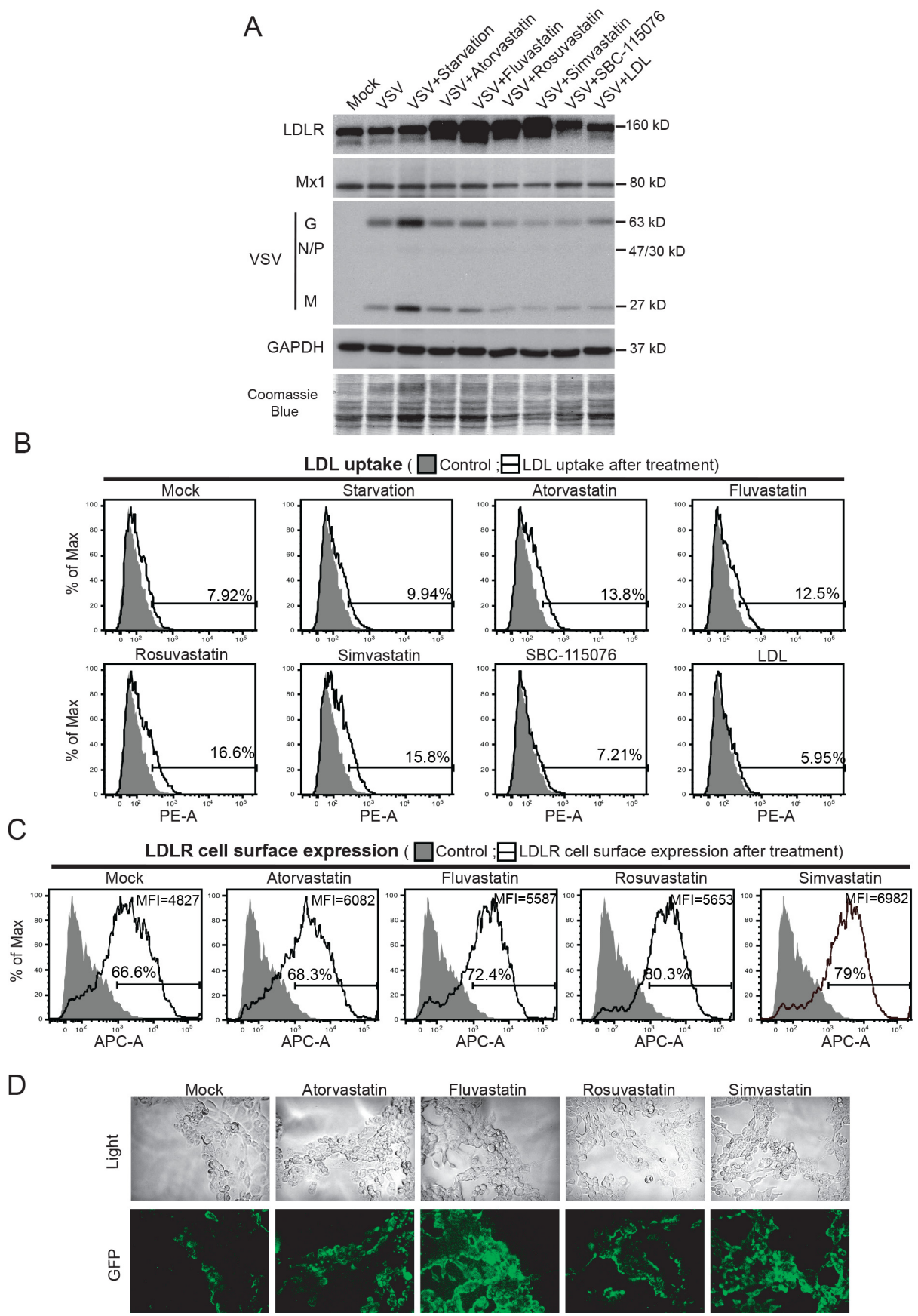1262 production) is represented.

1263

1264

A
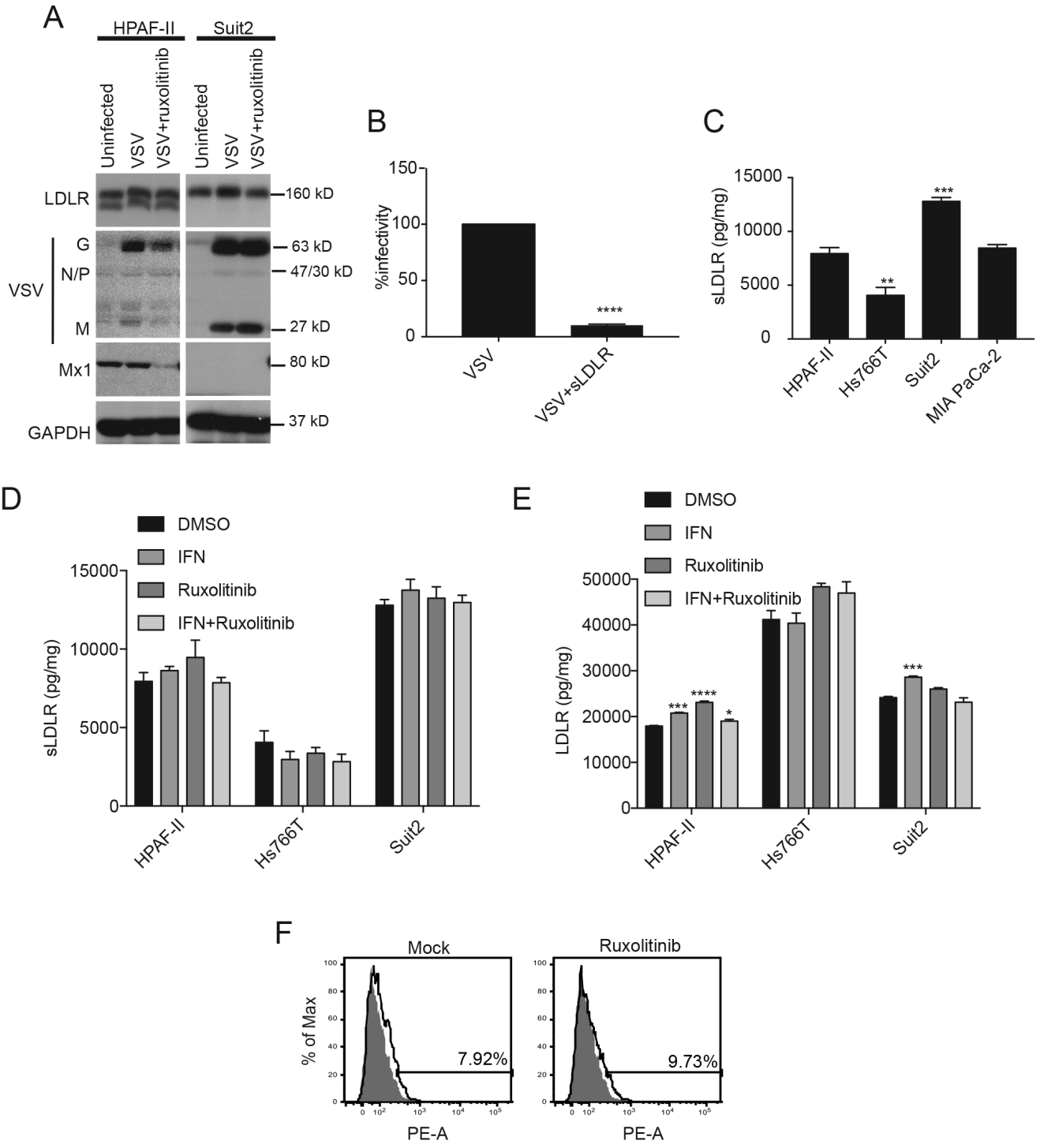
VSV attachment (■ Control ; □ VSV attachment)

B

A

| | HPAF-II | | | Suit2 | | |

LDLR — 160 kD

VSV — G — 63 kD
N/P — 47/30 kD
M — 27 kD

Mx1 — 80 kD

GAPDH — 37 kD

B

%infectivity

VSV   VSV+sLDLR
****

C

sLDLR (pg/mg)

HPAF-II   Hs766T   Suit2   MIA PaCa-2
**   ***

D

- DMSO
- IFN
- Ruxolitinib
- IFN+Ruxolitinib

sLDLR (pg/mg)

HPAF-II   Hs766T   Suit2

E

- DMSO
- IFN
- Ruxolitinib
- IFN+Ruxolitinib

LDLR (pg/mg)

HPAF-II   Hs766T   Suit2
*** **** *   ***

F

Mock   Ruxolitinib

% of Max

7.92%   9.73%

PE-A   PE-A

Treatment Group

VSV characteristics

VSV alone

Low attachment
Low replication
Low production

VSV + ruxolitinib

Low attachment
High replication
High production

VSV + polycation

High attachment
Low replication
Low production

VSV + ruxolitinib + polycation

High attachment
High replication
High production

Cancer Cell

VSV infected cancer cell

VSV Virion attachment

VSV-Encoded Foreign Protein (GFP)

VSV Virion production